Title
THE SPECTRA OF ARTICLES EMITTED FROM HEAVY ELEMENTS BOMBARDED BY 31 MeV PROTONS

Author
Igo, George J.

Publication Date
1953-06-01

UNIVERSITY OF CALIFORNIA

Radiation Laboratory

BERKELEY, CALIFORNIA

UCRL-2242
Unclassified-Physics Distribution

UNCLASSIFIED

cy 2

UNIVERSITY OF CALIFORNIA

Radiation Laboratory

Contract No. W-7405-eng-48

THE SPECTRA OF PARTICLES EMITTED FROM HEAVY ELEMENTS BOMBARDED BY 31-MEV PROTONS

George J. Igo
(Thesis)

June, 1953

Berkeley, California

TABLE OF CONTENTS

THE SPECTRA OF PARTICLES EMITTED FROM HEAVY ELEMENTS BOMBARDED BY 31-MEV PROTONS

George J. Igo

Radiation Laboratory, Department of Physics,
University of California, Berkeley, California

June, 1953

ABSTRACT

The energy distributions of inelastically scattered particles emitted by thin foils of Sn, Ta, Au, and Pb when bombarded by 30.7 Mev protons have been measured at five scattering angles. The spectra of inelastically scattered charged particles from the four elements at each deflection angle are quite similar in shape and in magnitude, and the peaks of the distributions fall at higher energies at small scattering angles. The angular distributions are strongly peaked forward. These results are in qualitative agreement with a nucleon-nucleon type process occuring on the rim of the nucleus. The inelastically scattered particles are mainly protons.

The differential cross section for elastic scattering is in agreement with an opaque-sphere model for the nucleus.

The distribution of energy losses of 30.7 Mev protons passing through a thin absorber has a full width at half-maximum of 50 percent and a high-energy tail, in agreement with the theory of Landau[45] and Symon.[46] A method has been developed to narrow the full width of the distribution to 35 percent and to eliminate the high-energy tail.

I. INTRODUCTION

A great amount of work has been done in recent years to investigate the forces of the nucleus. The evidence gathered from nucleon-nucleon scattering, meson production by nucleons and photons, and meson-nucleon scattering experiments has given a concept of the forces between elementary particles. This concept must be compatible with the results of nucleon-nuclei scattering experiments. Also the scattering of nucleons by complex nuclei leads to models for the nucleus.

Evidence for nuclear models comes from measurements of the total neutron cross sections of nuclei. They have been investigated at 14 Mev[1], 25 Mev[2], 40 Mev[3], 84 Mev[4], 95 Mev[5], and at 270 Mev[6,7]. Measurements at 90 Mev showed effects interpretable in terms of nuclear transparency[8], while measurements at 25 and 14 Mev can be interpreted in terms of an opaque nucleus. In order to account for the neutron cross sections over the full energy range from 14 Mev to 270 Mev, Jastrow[9] and Roberts assume that the density of nucleons in the nucleus is uniform within a region whose radius increases roughly as $A^{1/3}$. Outside this core, however, a diffuse region exists in which the nucleon density falls off in a distance approximately equal to the range of nuclear forces. At moderately low energies the diffuse tail is opaque. For light elements the increase in cross section due to the tail is larger, relatively, than for heavy elements. At higher energies the diffuse tail does not contribute appreciably to the cross section, and the cross section remains flat. Another effect of the diffuse region is destruction of the diffraction pattern in the elastic cross sections of the light elements, though only blurring slightly the diffraction patterns of the heavy elements.[10]

Evidence for the shape of the nuclear well comes from measurements of the momentum distributions of the nucleons. The momentum distributions of nucleons in carbon, deuterium, and oxygen nuclei have been inferred from the energy distributions of the protons obtained at various angles when 340 Mev protons are incident on these nuclei.[11]

Protons obtained from carbon and oxygen have energy spectra that are consistent with the use of a Gaussian nucleon momentum density distribution having a 1/e value corresponding to a nucleon energy of 16 ± 3 Mev.

The energy levels of light nuclei have been investigated through the inelastic scattering of protons on these nuclei.[13-32] The experiments have been done at moderate energies (5 to 32 Mev), and are limited to light nuclei where the coulomb barrier is not too high for de-excitation of the nucleus by charged-particle emission to compete favorably with neutron emission.

In order to study the heavy elements, the inelastic scattering of neutrons has been observed.[34-39] Graves and Rosen[33] have studied the neutron inelastic energy spectra from Al, Ag, and Bi bombarded with 14 Mev neutrons. They find the number of emitted neutrons per unit energy interval appears to be Maxwellian in the region 0.5 to 4.0 Mev, which is in agreement with the statistical theory of the compound nucleus.[40] In developing the statistical theory of nuclear reactions the assumption is made that the mode of disintegration of the compound nucleus depends only upon the excitation energy and angular momentum and is independent of the method of formation. This implies that the neutron spectra from (p, n) reactions should not differ appreciably from the energy distributions of neutrons from (n, n) processes, provided the compound nuclei and their excitation energies are the same. Gugelot[41], using 16 Mev protons, has measured the temperatures of residual nuclei as a function of the atomic number. The temperature of the nucleus resulting from a (p, n) event is compared with the temperature of the same residual nucleus formed by an inelastic neutron event at 14 Mev measured by Graves and Rosen. It is found that the temperatures are in agreement.

According to the statistical theory, the inelastic scattering of protons from heavy elements at 32 Mev would be small because the high coulomb barrier makes de-excitation by neutron emission most probable. At 90 degrees the differential cross section for Pb would be about 1 millibarn. Britten[32] measured the differential cross section of Pb and found it to be considerably larger than this. Furthermore the inelastic scattering spectra were fairly flat and did not show a Maxwellian distribution with a peak at the energy corresponding to the nuclear temperature. The work described here is a further investigation of the charged particles emitted by heavy elements when bombarded by 30.6 Mev protons.

II. DESCRIPTION OF THE EXPERIMENT

The linear accelerator accelerates a beam of protons to 30.7 Mev and a small number of H_2^+ ions to 15.4 Mev. The beam is all included in an area of less than 1/4 inch by 1/4 inch as it leaves the linear accelerator. Alvarez[42] has shown that under certain operating conditions it has a RMS energy width of less than 100 Kev. In order to eliminate the H_2^+ ions from the beam, a thin stripping foil (Fig. 1) is placed at the exit end of the linear accelerator and the 30.6 Mev proton beam is deflected through 20 degrees by a steering magnet. The stripping foil is necessary because the H_2^+ ions and the 30.7 Mev protons have the same $H\rho$ value. The beam is clipped to 1/4 inch by 1/4 inch by the second collimating aperture. It passes through a three carbon disc collimator designed to remove protons that have suffered energy degradations in slit penetrations. The protons pass through a thin target foil on the central axis of the scattering chamber and then into a Faraday cup which monitors the beam. (Figure 2a).

The counters are mounted on a table inside the scattering chamber. (Fig. 2b). The table can be rotated by means of a selsyn drive mechanism which can be controlled in the counting area. The target mechanism is also remotely controlled. The scattering chamber is evacuated during the experiment. Target-in and target-out runs may be made interchangeably, and the target may be selected from a group of five targets without breaking the vacuum. During a 144-hour run, in which one-half the data were obtained, it was not necessary to open the scattering chamber. Therefore an optimum use of the proton beam could be made.

It was necessary to measure the energy and determine the types of particles emitted by thin foils made of heavy elements. Counters were preferred to plates or cloud chambers because of the necessity of measuring a large number of spectra. The final data involved twenty spectra, each of about three thousand measured particles. Several detection methods measure momentum with a magnetic field and one other quantity such as the time of flight, energy, range, or specific ionization. Because of the bulk of the magnet it seemed desirable to use other methods. The combination of specific ionization and range necessitate the examination of a group of particles with small range differences. The measurement of energy and specific ionization seemed the best because particles of all energies from the lowest observable to 30.7 Mev may be examined simultaneously. Thus the information can be taken at an optimum rate. In some of the work, small energy intervals were examined because it was necessary to pulse height analyze the specific ionization pulses of the particles in this energy interval, but in later work a pulse-height analyzer was used to obtain the energy spectra.

To increase the counting rates, thick targets are desirable. The thickness is limited by the multiple scattering suffered by the photons passing through the target. The root mean square angle of multiple scattering was kept small enough to insure that the proton beam would all be collected in the Faraday cup. A second limitation on the thickness of the target is the requirement that the lowest energy heavy particles emitted by the target should not lose a large fraction of their energy in the target. Preliminary experiments indicated that there were no heavy charged particles emitted by the targets with energies of less than the order of the Coulomb barrier heights, or about ten Mev on the average for the elements examined. The targets were thin enough so that 10 Mev protons would lose less than two Mev in the target. This introduces an uncertainty of this amount in the Coulomb barrier cutoff energy in the observed spectra.

The counter telescope consisted of three proportional counters, which would give an accurate measurement of the average specific ionization, followed by a scintillation counter. In the following discussion, the three proportional counters are referred to as a "triproportional counter". (Fig. 2b).

A particle, in order to be counted, must pass through the thin triproportional counter, which thereupon registers a pulse whose height is linearly proportional to the specific ionization of the particle. The particle stops in the scintillation counter where it registers a pulse height linearly proportional to the energy and independent of the type of the particle.[43] The observation of these quantities yields the energy and the mass of the particle which has passed through the counter telescope. The counter data were analyzed by electronic and photographic methods. Final results are expressed in the form of energy spectra. Data were collected at six scattering angles in the investigation of each of four heavy elements.

III. THE PROTON BEAM: METHOD OF USE

Collimation

The method of collimating the beam is described in Section II. The collimator mentioned there consists of a 1/8-inch drilled carbon disc followed by two 3/16-inch drilled carbon discs spaced a foot apart on a common axis. The collimation of the beam is done by the 1/8-inch disc. The other carbon discs remove scattered particles from the beam.

The collimating system is identical to that used by Benveniste and Cork[44] in their investigation of scattering in helium. Figure 3 shows the helium range spectrum at a scattering angle of 30 degrees. The particles lying between the elastically scattered alpha peak and the elastically scattered protons could be due to beam contamination. If this were so, then an appreciable part of the 15 and 30 degree inelastic scattering spectra observed in the present work (Fig. 6) could be due to beam contamination. The contribution to the differential cross section at angles larger than thirty degrees would be small, because the ratio of inelastically to elastically scattered particles increases with the azimuthal angle.

Alignment of Equipment

To align the equipment, the collimator (D, Fig. 1) is first removed by lifting it into another section of the collimator housing. The position of the uncollimated beam is determined at the rear of the scattering chamber by burning a spot on a piece of glass which is placed between the scattering chamber beam exit and the integrator H. The beam line is defined by the aperture C and the beam spot. The integrator is removed from the equipment after first letting the collimator and scattering chamber up to atmospheric pressure. Next a transit is aligned along the beam line. The collimator D is dropped back into position and aligned along the beam line. The scattering chamber beam entrance and exit ports are similarly aligned. The scattering table is run around to 180 degrees, the triproportional counter is removed and the scintillation counter is checked for alignment. The triproportional counter is replaced and the system is pumped down. As a check on the alignment, a piece of glass is placed in one of the target positions and lowered into beam position. After a short exposure, if the system is properly aligned, a well defined brown spot is made on the glass.

Integration

The beam was collected in a Faraday cup* with a 1-1/2 inch opening to minimize losses from multiple scattering. A permanent magnet located at the opening prevented entry of ionization electrons from the target, and another permanent magnet located back of the opening prevented

---

* The Faraday cup was designed and made by Gerhard Fischer.

secondaries formed in the Faraday cup from escaping. The cup is connected by a coaxial cable to a capacitor calibrated to within 0.1 percent. The capacitor voltage was read by a feedback electrometer circuit which makes the effective cable capacity negligibly small. The electrometer output was recorded on a Leeds and Northrup recording millivoltmeter.

Beam Intensity

The beam intensity was limited by several factors. The first of these was the accidental counting rate, which should not be larger than the real counting rate. Since a fourfold coincidence was demanded in order for a particle to be counted as coming from the target, this did not limit the counting rate. Pile-up in the individual counters was held to two percent. The limiting factor was the fluctuation of the base line in the linear amplifiers. The linear amplifiers tend to undershoot when large pulses are fed in; when the counting rate is rapid the base line can be depressed for a considerable percentage of the time. The counting rate had to be kept down to minimize the undershoot. The criterion for the beam intensity was that the elastic peak counting rates before and after coincidence with the triproportional counter should not differ by more than four percent. Only a negligibly small number of pulses due to particles not originating in the target had pulse heights comparable to the elastically scattered particle pulse height.

In a typical run it was necessary to adjust the beam flux with the pre-steering magnet collimator (A, Fig. 1) so that the total counting rate due to all heavy, charged particles in each counter was two counts per beam pulse (approximately 300 microseconds). The magnitude of the beam flux depended on the scattering angle under observation. At large scattering angles the average current was about 10^{-9} amperes; at an angle of thirty degrees, about 5×10^{-11}. On days when the linear accelerator beam flux was large, the backward angles were obtained; and, conversely, the forward angles. In this manner, practically all the obtainable beam could be used.

Beam Energy*

The range of the protons from the linear accelerator in aluminum was measured. An aluminum absorber 1025 milligrams per cm^2 thick (over 90 percent of the range of a 30 Mev proton) was placed inside the Faraday cup manifold at a distance of two inches from the Faraday cup opening to minimize multiple scattering corrections. A positive voltage of two hundred volts was placed on the absorber to prevent ionization electrons from entering the cup. Outside the manifold a variable absorber ranging from 0 to 1000 milligrams per cm^2 of aluminum could be placed in the beam. The energy of the beam was found to be 30.7 ± 0.6 Mev.** The steering magnet current meter reading was noted. In experimental runs, small corrections to this value could be made if the steering magnet current was slightly different from its value when the measurement was made. The magnetic field was assumed to be linearly dependent on the magnet current for small changes in the current reading.

IV. THE COUNTERS

The Scintillation Counter

The scintillation counter consists of a 3/8 inch by 3/8 inch by 1 inch piece of thallium activated sodium iodide crystal mounted on the top of a 3/8 inch quartz light pipe in the shape of a truncated cone with the base ground to fit the light-sensitive surface of a 5819 photomulitplier. The crystal, light pipe, and photomultiplier light-sensitive surface were cemented together with a cold-setting compound which has good light transmission properties in the visible region of the spectrum, does not attack sodium iodide, and hardens to give good tensile strength. The compound is called Bonder R-313***. The crystal and light pipe were covered with a 1/4 mil aluminum foil to increase the light-collecting efficiency. The crystal was cleaved and mounted in a dry box. It was

---

* The measurement of the beam energy was made by Byron Wright.

** The range energy curves of Aron, Hoffman, and Williams, AECU 663 were used. The Al range curve may be incorrect by 1 percent according to Byron Wright, of the University of California Radiation Lab.

*** Made by Carl H. Biggs Co. Los Angeles, California.

enclosed in the photomultiplier housing with a drying agent, phosphorus pentoxide, and the housing was pumped down to a good vacuum. Under these conditions a crystal lasts indefinitely. The resolving power, determined from the pulse height distribution of elastically scattered particles from Pb, had a full width at half maximum of five percent.

The Triproportional Counter.

The triproportional counter consists of three cylindrical counter units, 3/4 inch in diameter and five inches long, in tandem, preceded by an identical unit. The dimension perpendicular to the course of particles scattered from the target is kept as narrow as possible to allow the counter telescope to look at small and large angles of scattering without getting in the path of the proton beam. The center wires were cleaned with a lint-free cloth and examined under a microscope for dust particles. The counter was constructed of low vapor pressure materials, thoroughly outgassed, and filled with a water-free mixture of 96 percent argon and 4 percent carbon dioxide. The voltage on the center wire was 1800 volts during a run. At any time the voltage could be lowered to 1400 volts, where the pulses from passing particles are barely discernible. Then the pulses from internal alpha sources could be detected. The sources are mounted in collimators which insure that all the alpha particles that enter the active region of the counter are stopped and so deliver their full energy in the counter gas. The Landau effect discussed in Section X does not apply because a definite total energy is imparted to the counter gas electrons by the alpha particle. The only statistical variations in the pulse height are due to the division of energy into ionization and excitation. The observed alpha particle pulse distributions had a full width at half maximum of five percent.

The number of alpha particles entering the active region was necessarily small, because at normal voltages for counting passing particles, they saturate the amplifiers. When this happens the amplifiers have a dead time of several hundred microseconds, which contributes an error to the total cross sections. The first unit is not used for data collection since it "sees" ionization electrons given off by the entrance foil. In addition it sees a flood of ionization electrons originating in the target. An investigation of these electrons was made. They could be deflected out of the counters with a small electromagnet, and the cross section for them was found to be of atomic dimensions. Neither these electrons nor the ones formed in the entrance window enter the three units which measure the specific ionization, since the electrons multiple-scatter through large angles in the first unit.

V. ELECTRONIC ARRANGEMENT

A diagram of the electronic equipment is shown in Fig. 4. Pulses from the triproportional and scintillation counters were clipped and shaped so that they were two microseconds long and reasonably flat on top. They were suitably amplified by preamplifiers located close to the counters and by amplifiers located in the counting area. The outputs of the triproportional counter amplifiers feed a Rossi-type coincidence circuit which selects the smallest pulse. The coincidence output was fed into a multichannel integral pulse-height analyzer. The output of the scintillation counter amplifier was fed into a single-channel differential pulse-height analyzer. The outputs of both pulse-height analyzers were fed into coincidence circuits. In another channel one output is delayed before coincidence to measure the accidental counting rate. As a monitor on the single-channel pulse-height analyzer output, an integral counting rate was measured on the pulses in the scintillation counter due to inelastic particles.

An eight-channel differential pulse-height analyzer was installed after the first run. It was decided to run a check on the data obtained in the previous run. Figure 5 is a diagram of the electronic equipment. The first run had indicated that the spectra were mainly protons. Therefore the necessity of running discriminator plateaus on the triproportional counter pulses was eliminated. The triproportional counter served to determine that a heavy, charged particle had passed through. The requirement was met by demanding that the specific ionization pulse from the triproportional counter be as large as or larger than that of a 32-Mev proton, and that it be in fourfold coincidence as in the previous run. The output of the scintillation counter amplifier fed the eight-channel differential pulse-height analyzer, and the outputs of the triproportional counter amplifiers, after passing through a Rossi-type coincidence circuit, was used to gate the pulse-height analyzer "on". The elastic peak counts were monitored before and after coincidence to insure that the counting rate was not too high. Accidentals were measured in another channel. As a qualitative check on the identification of the particles, a photographic method was employed to determine the mass of the particles: the specific ionization is proportional to the mass/energy, so the product of the scintillation counter and the triproportional counter pulse-heights is proportional to the mass of the particle. The pulses from the counters were displayed on the vertical and horizontal plates of an oscilloscope. The oscilloscope beam was gated on by the proportional counter output since the counting rate was smallest in that counter. The resulting distributions were photographed (Figure 25). Particles of different masses should fall on separate hyperbolae which should be discernible if the particles occur in appreciable numbers.

VI. ANALYSIS OF THE GEOMETRY

The collimated beam strikes the target in an area of about 1/4 inch by 3/16 inch. The scattered particles enter the counter telescope through a 3/32 inch diameter collimator placed 5-1/2 inches away from the target. The apertures in the triproportional counter are 1/4 inch in diameter; in the exit window, 3/8 inch; and in the entrance window of the scintillation counter, 1/2 inch, so as to minimize losses due to multiple scattering. An order-of-magnitude calculation shows that the multiple-scattering loss of protons of the lowest energy observed, about 8 Mev, is a few percent. Protons of higher energies multiple-scatter less, so the correction is small.

$d^2\sigma/dEd\Omega$ was calculated using the following values for the measured quantities:

N_p	number of protons in beam
N_n	number of nuclei/cm^2 in the target
$N_{\Delta E}$	number of counts/energy channel
n	number of protons/coulomb
η	grams/cm^2 in target
E	channel width in Mev
$\Delta\Omega$	solid angle observed by counter
Q	charge collected in Faraday cup
a	Avagadro's number
A	atomic weight of target element
θ	target angle between the beam line and the normal to the target: 45°

$$N_n = \frac{\eta\ a}{\sin\theta \times A} = 9.62 \times 10^{-23}\ \eta/A$$

$$N_p = Qn = CVn = 6.35 \times 10^{10}\ V$$

$$d^2\sigma/dEd\Omega = \frac{N_{\Delta E}}{N_n N_p} \frac{1}{\Delta\Omega\ \Delta E} = 6.5 \times 10^{-6}\ N_{\Delta E} A/\ nV \frac{\text{millibarns}}{\text{steradian} \times \text{Mev}}$$

VII. LINEARITY OF EQUIPMENT

As a check on the linearity of the equipment, the spectrum of particles emitted by a carbon target has been measured. The spectrum is shown in Fig. 7. The abscissa has been corrected for window absorption, which amounted to 31 milligrams/cm^2 of aliminum. The incident energy has been measured 30.7 Mev. In plotting the data, 30.7 Mev was assumed to correspond to the maximum of the pulse-height distribution of the elastically scattered particles from Pb. The spectrum is in good agreement with the spectrum of Levinthal et al.[31] Their measurements were made by exposing emulsions to the scattered particles.

VIII. REPRODUCIBILITY OF DATA

As a check on the reproducibility of the spectra, spectra of Pb at 90 degrees are presented in Figs. 8 and 9. The data shown in Fig.

8 were obtained in October, 1952 with counting equipment which was not used in subsequent runs. At that time the scattering chamber had not been placed in the bombardment area, and an older chamber was used. Because of the small size of the older scattering chamber, the counters were placed outside, and therefore a larger window correction had to be made to the energy of the particles. The spectra differ in that the cutoff energy is higher in the later data (Fig. 9). This is attributable to the energy spread contributed to low-energy protons by the larger window absorber in the earlier work.

IX. PROCEDURE

The procedure for an experimental run usually followed the same pattern. First the position of the beam was determined, and all the equipment was aligned with respect to the beam line. The procedure has been described in Section II.

To insure that the counters were functioning properly, the pulse-height distribution of elastically scattered particles from a heavy element was examined. If the scintillation counter was functioning properly, the peak would have a full width at half maximum of about five percent. The triproportional counter unit counter amplifiers were adjusted in gain so that the pulses from internal alpha sources were of equal height in unit counters two and three and 20 percent higher in unit counter one. These settings had been previously determined by photographing the Landau distribution from each unit counter and adjusting the gains so that the peak of the ionization distribution in each counter had the same height. Another way to check the settings of the linear amplifiers was by running pulse-height distributions with the eight-channel pulse-height analyzer. Both methods gave the same settings for the linear amplifiers. The electronic arrangement was tested with artificial pulses during the experiment several times. When data were to be taken the beam intensity was adjusted so that the counting rates of elastic particles before and after coincidence with the triproportional counter output were within four percent of each other, since this was the criterion for the beam intensity (Section II). Individual runs varied in length because the cross section decreased in the backward directions. The spectra were run several times at any given angle to minimize errors due to changes in the gains of the equipment or due to human mistakes. Target-out runs were made at frequent intervals but no counts in any channels were obtained. The runs were made for a predetermined amount of beam flux as measured by the charge collected in the Faraday cup.

X. USE OF PROPORTIONAL COUNTERS IN THE MEASUREMENT OF IONIZATION

Useful methods of identifying particles of different mass often involve a measurement of specific ionization and some other parameter such as momentum, energy, or range. These schemes require a counter of small stopping power and good proportionality to measure the ionization. It has often been assumed that a gas proportional counter admirably satisfies these requirements, on the assumption that the statistical fluctuations in the energy loss of the particles traversing the counter are governed by the statistical fluctuations in the number of ion pairs, as calculated on the basis of about 25 electron volts per ion pair. Experiment and theory of Landau[45] and of Symon[46] indicate, however, that the fluctuations are considerably larger.

In order to check the Landau and Symon theory, protons of 30.7-Mev energy from the linear accelerator were scattered elastically from a 0.00025-inch Pb target through a triproportional counter and stopped in a scintillation counter. Both counters have been described in detail in Section IV. The elastic protons were separated by means of a single channel pulse-height analyzer fed from the scintillation counter, and the output of the analyzer was used to trigger the sweep of an oscilloscope; the triproportional counter pulses after amplification and suitable delay were applied to the vertical plates. The oscilloscope screen was photographed on moving film read on a microfilm viewer. The stability and linearity of the system had been shown to be reliably good in previous work.

The three amplifiers fed by the triproportional counter were adjusted in gain so that the collimated internal alpha-particle sources gave pulses of the same height. It was assumed that the gains of the three proportional counters were identical. Since the alpha pulses are well collimated and extremely monochromatic, they lose a definite amount of energy in the counter and show a well-defined pulse height. Since the geometry of the counters and the alpha sources are identical, any differences in the gain settings of the linear amplifiers are due to differences in the gains of the delay line clippers and the preamplifiers. However, a check was made on the gains of the triproportional counter, and they proved to be very close. Minor adjustments have been made in the gains to improve the equality in later experimental use of the counters.

Figures 10, 11 and 12 show graphs of pulses from the three units of the triproportional counter. The pulse-height distributions have been observed to be independent of beam intensity, thus indicating that no significant part of it is due to pile-up. A theoretical curve has been computed from the formulas and curves of Symon. Since the counters are identical, the same theoretical curve applies to all three units. For comparison with experiment, both the theoretical curve and the experimental points were plotted on logarithmic graph paper; the best fit by eye gave scaling factors for both coordinates. The solid curves are the resulting theoretical distribution; no additional factors introducing spread have been folded in. The theoretical values of average total energy loss and of maximum energy loss by a 30.7-Mev proton in a single collision with an electron are shown. For comparison there is also shown a Gaussian distribution about the average of the width determined by statistics on the number of ion pairs formed at 25 electron volts per ion pair. The Gaussian curve is normalized to the same height as the Landau distribution.

The surprisingly broad distributions with high-energy tails are due to the non-negligible probability of collisions in which the charged particle imparts large kinetic energy to the electron. This reduces radically the number of primary collisions, thus increasing the width of the statistical distribution, and in addition gives rise to the high energy tail. Note in Figs. 10, 11 and 12 the maximum allowable energy loss in a single collision is, in this particular case, approximately twice the average total energy loss of the proton in the counter. This is in sharp contrast to the very narrow pulse-height distributions that have been observed when the charged particle expends its entire track in the counter. The statistical fluctuations are due only to the variations in the ratio of energy loss in ionization to energy loss in excitation.

The outputs of the triproportional counter amplifiers feed a Rossi-type coincidence circuit. The output of a Rossi circuit is equal to the smallest of the input pulses if the three pulses are in coincidence. The smallest pulse was displayed on an oscilloscope triggered, as before, by the single-channel pulse-height analyzer fed by the scintillation counter. A graph of 400 pulses is shown in Fig. 13. The distribution approximates a Gaussian distribution with a full width at half maximum of thirty five percent. The high-energy tail observed in the individual proportional counter distribution has disappeared and the distribution is narrower. Such a distribution of pulse can be used in experiments in which the mass of the particle is to be identified by a measurement of the specific ionization and one other parameter such as the energy, momentum, or range. It will be noticed that the average pulse height in the three unit counters did not fall at the same height. There was about a fifteen percent difference in the overall gains of the three unit counters, which indicates that the gain setting is not critical. The solid curve is a theoretical distribution for the smallest pulse. The theoretical curve and the experimental data were plotted on logarithmic graph paper and the best fit by eye gave scaling factors for both coordinates. The theoretical expression for the curve is $p' = np\,(1 - \int_0^E p\,dE)^{n-1}$*, where p is the Landau distribution for 30.7-Mev protons that have passed through a unit counter, n is the number of times the Landau distribution is measured,

* The expression was derived by Bayard Rankin, of the University of California Radiation Laboratory.

and p' is the distribution of the smallest of the n pulses. n in this case was three.

It is interesting to note that the narrow distribution could not be obtained by using a counter with three times the stopping power of each unit proportional counter. A calculation shows the distribution of energy losses suffered by a charged particle passing through the counter would be very similar to the distribution from the unit proportional counters. The narrow distribution is obtained as a consequence of taking the smallest pulse from the three unit proportional counters. Effectively the energy loss distribution is sampled three times. Advantage is taken of the relatively steep rise of the energy loss distribution on the low energy loss side and the gradual fall off on the high energy loss side, so that the smallest energy loss is quite close to the most probable energy loss.

XI. RESULTS

Figure 14 shows the energy spectra of particles emitted at 90 degrees by thin targets of Pb (A = 208), Au (A = 197), Ta (A = 181), and Sn (A = 120). The distributions centered at 30.7-Mev are those of the elastically scattered protons, and the lower energy components of the spectra are the inelastic contribution. Figures 15, 16 and 17 show the spectra at different angles to the proton beam. The inelastic-scattering parts of the spectra of the four elements are quite similar in shape and in magnitude at each of the five angles. Figure 19 shows the inelastic spectra of Sn at five representative angles. The maxima of the spectra shift toward higher energies at smaller angles, and the magnitude of the cross section increases in the forward direction. Figures 20, 21 and 22 bear this out for the other element.

All the protons that strike the center of the nucleus, where the mean free path is of the order of 1/12 of the Pb nuclear diameter, should form a compound nucleus. This has been born out experimentally by Ghoshal,[47] who has shown the theory of compound nucleus applied to reactions at a bombarding energy of 30 Mev. He studied the ratio: $\sigma(p, n)$: $\sigma(p, 2n)$: $\sigma(p, pn)$ on Cu^{63} and the ratio: $\sigma(\alpha, n)$: $\sigma(\alpha, 2n)$: $\sigma(\alpha, pn)$ on Ni^{60}. The ratios of the cross sections were found to be equal, giving a direct verification of the theory of compound nucleus. The work of other experimenters[31, 32] has been based on the assumption that the theory applies at these energies. Also theoretical distributions of particles as predicted by the compound-nucleus theory differ considerably from the observed spectra.[40] The spectra indicate that the process is probably a nucleon-nucleon one. The incident protons which have a De Broglie wave length (λ) of 5×10^{-13} cm; chip nucleons off the periphery of the nucleus. The proton is localized well enough so that it may interact with single nucleons on the periphery. Jastrow[9] has suggested that the work of Richardson et al[10] on elastic scattering and the work of DeJuren and Moyer[48] on the cross section for neutrons (described in Section I) could be interpreted if one assumed the nucleus is surrounded by a diffuse region, of thickness equal to the range of nuclear forces, in which the density of nuclear matter falls to zero. Such a diffuse layer would bring the results of this experiment into agreement with the nuclear model. In fact if the nuclear density cutoff were very sharp the total cross section for a nucleon-nucleon event would be of the order of one millibarn whereas the observed total cross section is about 0.3 barns. The shapes of the spectra are in agreement with a nucleon-nucleon type collision in that the maxima of the distributions are located at higher energies at the forward angles. The work of Cladis et al[11] on the interaction of 340 Mev protons with carbon has been interpreted by Wolff[12] as a nucleon-nucleon type process. The peaks of the spectra are observed to shift toward lower energies at larger angles. Also the neutron spectra of Hoffman and Strauch[49], observed when 95-Mev protons interact with Pb, Cu, and Al, rise to a maximum at lower energies for larger angles. The fact that the inelastic differential cross sections (Figs. 14, 15, 16 and 17) are almost the same for the four elements is in agreement with a nucleon-nucleon process, since the boundary of the nucleus increases slowly with the atomic weight ($A^{1/3}$ dependence).

Sources of Error

The experimental points in Figs. 14-18 show the standard errors due to statistical fluctuations. The errors were calculated on the number of counts in the pulse-height analyzer channels, except for the three lowest of the sixteen channels, for each energy spectrum. In the three lowest channels there were appreciable accidental counts. Figure 26 shows a typical spectrum. Curves have been drawn to show the counting rate in the scintillation counter, the accidental counting rate, the total counting rate, and the counting rate minus accidentals. No counts were observed in any of the channels in target-out runs. In the bottom three channels the statistical error of the subtracted data was calculated in the normal fashion.

A certain number of the lowest-energy protons would not be detected, because they could multiple-scatter into the walls of the counter. It is estimated that only a few percent of the lowest-energy protons are lost.

Another nonstatistical source of error lies in the elastic scattering of protons whose energy has been degraded by encounters with the collimating apertures. The differential cross section for coulomb scattering is proportional to $1/E^2$; therefore these particles scatter efficiently and would contribute to the inelastic-event spectrum. Slit scattering of the elastically scattered particles could occur at the entrance aperture of the counter telescope, and at forward angles could contribute appreciably to the inelastic-event spectra. It was found that the slit scattering from a carbon collimator was large, and this was attributed to the large area in cross section along the path of the scattered beam. A steel collimator was found to slit-scatter appreciably less. The spectrum of particles emitted from Pb at 15 degrees is shown in Fig. 6. If it is assumed that all inelastically scattered particles in the spectrum at 15 degrees are energy-degraded protons elastically scattered from the target, or protons suffering energy losses from slit scattering in the entrance aperture of the counter telescope, then approximately two-thirds the inelastic-scattering observed at 30 degrees could be unreal. (This amount was determined by taking the ratio of inelastic to elastic scattering at the two angles.) The effect is smaller at larger angles because the elastic-scattering cross section decreases. At 45 degrees, it amounts to 20 percent; and in the 60-degree spectra, five percent. At 90 and 135-degrees, the effect is negligible. Since part or all of the inelastic-scattering spectrum observed at 15-degrees could be due to real inelastic events, no attempt was made to subtract off parts of the spectra.

Another source of error is in the measurement of the distance of the collimating aperture of the counter telescope from the target. The distance is 5-1/2 inches ± 1/8 inch. No attempt was made to measure the distance any closer than 1/8 inch because the target holder could shift in position by this amount. This possible shift contributes a 4 percent error to the cross section measurements.

The energy of the beam is quite sensitive to the adjustment of the end drift tubes. The energy can shift slightly when the beam flux is maximized by the crew. But since the cross section is energy-insensitive, the shift introduced no appreciable error.

Elastic Scattering

The differential cross section for elastic scattering for the four elements examined is plotted as a function of angle in Fig. 23. Pb, Ta, and Au data can be fitted to a smooth curve. The differential cross section for Sn takes a dip at 45 degrees. In Fig. 23 the diffraction pattern formed by plane waves of the De Broglie wave length of 31-Mev protons incident on the Sn nucleus have been plotted.[50] The assumption that the Sn nucleus acts like a completely opaque disc is a good one, since the mean free path in the nucleus is small for 31-Mev protons. The fact that no minima were observed for Au, Pb, and Ta was to be expected since the first minima should occur at 30 degrees where the cross section for Coulomb scattering is still large - about two barns for Pb. The radii of the nuclei were taken from the paper of Fernbach, Serber, and Taylor.[8]

The errors indicated in Fig. 23 are larger than statistical and are due to other causes. The statistical errors range from 0.1 percent for the 15-degree data to 10 percent for the 135-degree data. The errors in the forward directions are upper limits on the loss caused by slit scattering. The source of error in the 90-degree and the 135-degree data arises from the difficulty in determining what part of the distribution is elastically-scattered particles (Figs. 14 and 17). This could amount to a 25 percent error. The error at the forward angles amounts to 10 percent.

Some elastic scattering was studied by Britten.[32] He deduced a cross section for Pb at 90 degrees of 6.8 ± 1 millibarns - in good agreement with the 90-degree point in this work. Elastic scattering at higher energies has been investigated by Bratenahl et al[51] who examined the diffraction of 190-Mev neutrons by Be, C, Al, Cu, and Pb. Their results at larger angles fit the predictions of the transparent-nucleus theory. Richardson et al[10] found that the diffraction patterns of elastically-scattered particles resulting when nuclei were bombarded by 340-Mev protons indicate that the nuclei appear partially transparent. Amaldi et al[1], working with 14-Mev neutrons bombarding Pb, observed a strong forward peak with a minimum in the angular distribution at about 25 degrees and a small secondary maximum near 40 degrees. Assuming that the Pb nucleus behaved as an opaque sphere, they deduced from the position of the minimum that the radius of the Pb nucleus was about 10^{-12} cm. This value is larger than that deduced by Fernbach, Serber, and Taylor.[8] The disagreement may be due to the opaqueness to 14-Mev neutrons of the diffuse region surrounding the nucleus.

Identification of Particles

Figure 24 shows discriminator curves for particles of 31-Mev, 20-Mev, and 14-Mev energies from a Pb target at 60 degrees. The plateau moves out in a linear fashion, proportional to the inverse of the energy. Since at 31 Mev all the particles must be protons, then the other plateaus must be due to protons and not to deuterons in any large number. Five point discriminator plateaus were run on each 2-Mev energy channel. No deuterons were observed from any of the elements in large numbers. Any peaked distribution of deuterons would have been observed, and if the deuterons were distributed uniformly at all energies, they must not represent more than 20 percent of all particles counted. Figure 25 shows some of the film data. The hyperbolas can be discerned. No large number of counts lie off the proton hyperbola. The elastic-scattering peak is identified by the large amount of blackening, and the Coulomb cutoff for the protons can be seen.

Summary of Conclusions

1. The energy distribution of inelastically scattered particles emitted by thin foils of Sn, Ta, Au, and Pb when bombarded by 30.7-Mev protons have been measured at five scattering angles. The spectra of inelastically scattered charged particles from the four elements at each deflection angle are quite similar in shape and in magnitude, and the peaks of the distributions fall at higher energies at small scattering angles. The angular distributions are strongly peaked forward. These results are not in agreement with a compound-nucleus theory. They are in qualitative agreement with the theory of a nucleon-nucleon type process occuring on the rim of the nucleus.

2. The inelastically scattered particles are mainly protons.

3. The differential cross section for elastic scattering is in agreement with an opaque-sphere model for the nucleus.

4. The distribution of energy losses of 30.7-Mev protons passing through a thin absorber has a full width at half-maximum of 50 percent, and a high-energy tail, in agreement with the theory of Landau[45] and Symon.[46] A method has been developed to narrow the full-width of the distribution to 20 percent and to eliminate the high-energy tail.

ACKNOWLEDGMENTS

The author is indebted to a great many people without whose contributions this research work could not have been accomplished.

In particular:

To Professor Luis Alvarez, who suggested the research problem, offered many valuable suggestions, and has been my teacher.

To Professor A. C. Helmholz, for aid and encouragement.

To Robert Watt, Wendell Olson, and the many members of the linear accelerator crew, who have done much beyond their duties.

To many members of the Electronics Group for their maintenance of the electronics equipment.

To Roy Marker, who designed the scattering chamber.

To Dr. Robert Eisberg, who was an associate in all of this work.

XII. REFERENCES

1. E. Amaldi, O. Bocciarelli, B. N. Cacciapuoti, and G. C. Trabacchi, Nuovo Cimento 3, 203 (1946).

2. R. Sherr, Phys. Rev. 68, 240 (1945).

3. R. H. Hildebrand and C. E. Leith, Phys. Rev. 80, 842 (1950).

4. L. S. Cook, E. M. McMillan, J. M. Peterson and D. C. Sewell, Phys. Rev. 72, 1003 (1947).

5. J. DeJuren and N. Knable, Phys. Rev. 77, 606 (1950).

6. J. DeJuren, Phys. Rev. 80, 27 (1950).

7. R. Fox, C. Leith, L. Wouters, and K. R. MacKenzie, Phys. Rev. 80, 23 (1950).

8. S. Fernbach, R. Serber and T. B. Taylor, Phys. Rev. 75, 1352 (1949).

9. R. Jastrow and J. E. Roberts, Phys. Rev. 85, 757 (1952).

10. R. E. Richardson, W. P. Ball, C. E. Leith Jr. and B. J. Moyer, Phys. Rev. 86, 29 (1952).

11. J. B. Cladis, W. N. Hess and B. J. Moyer, Phys. Rev. 87, 425 (1952).

12. P. Wolff, Phys. Rev. 87, 434 (1952).

13. R. Ely, A. J. Allen, J. S. Arthur, R. S. Bender, H. J. Hausman and E. M. Reilley, Phys. Rev. 86, 859 (1952).

14. R. H. Dicke and J. Marshall, Phys. Rev. 63, 86 (1943).

15. H. W. Fullbright and R. R. Bush, Phys. Rev. 74, 1323 (1948).

16. E. M. Reilley, A. J. Allen, J. S. Arthur, R. S. Bender, R. L. Ely and H. J. Hausman, Phys. Rev. 86, 857 (1952).

17. T. R. Wilkens and G. Kuerti, Phys. Rev. 57, 1082 (1940).

18. T. R. Wilkens, Phys. Rev. 60, 365 (1941).

19. E. M. Hafner, Ph.D. thesis, University of Rochester (1948).

20. E. H. Rhoderick, Proc. Roy. Soc. (London) 201, 348 (1950).

21. J. E. Brolley, M. B. Sampson and A. C. G. Mitchell, Phys. Rev. 76, 624 (1949).

22. K. K. Keller, Phys. Rev. 84, 884 (1951).

23. C. J. Baker, J. N. Dodd, and D. H. Simmons, Phys. Rev. 85 1051 (1952).

24. D. B. Cowie, N. P. Heydenberg and G. C. Phillips, Phys. Rev. 87, 304 (1952).

25. C. F. Powell, A. N. May, J. Chadwick and T. G. Pickavance, Nature 145, 893 (1940).

26. H. Heitler, A. N. May, and C. F. Powell, Proc. Roy. Soc. (London) 190, 180 (1947).

27. K. E. Davis and E. M. Hafner, Phys. Rev. 73, 1473 (1948).

28. H. E. Gove and J. A. Harvey, Phys. Rev. 82, 658 (1951).

29. E. M. Reilley, A. J. Allen, J. S. Arthur, R. S. Bender and H. J. Hausman, Phys. Rev. 82, 658 (1951).

30. C. Levinthal, E. Martinelli and A. Silverman, Phys. Rev. 78, 199 (1950).

31. R. Britten, Phys. Rev. 88, 253 (1952).

32. E. R. Graves and L. Rosen, Phys. Rev. 89, 343 (1953).

33. H. H. Barschall, M. E. Battat, W. C. Bright, E. R. Graves, T. Jorgensen and J. H. Manley, Phys. Rev. 72, 881 (1947).

34. H. H. Barschall, J. H. Manley and V. F. Weisskopf, Phys. Rev. 72, 875 (1947).

35. H. T. Gittings, H. H. Barschall, and G. G. Everhart, Phys. Rev. 75, 610 (1949).

36. D. D. Phillips, R. W. Davis, and E. R. Graves, Phys. Rev. 88, 600 (1952).

37. P. H. Stelson and C. Goodman, Phys. Rev. 82, 69 (1950).

38. B. G. Whitmore and G. E. Dennis, Phys. Rev. 84, 296 (1951).

39. V. F. Weisskopf and D. H. Ewing, Phys. Rev. 57, 472 (1940).

40. P. C. Gugelot, Phys. Rev. 81, 51 (1950).

41. L. W. Alvarez et al, AECU-120

42. W. Franzen, R. Peele, and R. Sherr, Phys. Rev. 79, 742 (1949).

43. J. Benveniste and B. Cork, Phys. Rev. 89, 422 (1953).

44. L. Landau, J. Phys. (USSR) 8, 201 (1944).

45. K. R. Symon, thesis, Harvard University (unpublished). Parts of this work appear in B. Rossi, High Energy Particles, (Prentice-Hall, Inc., New York, 1952).

46. S. N. Ghoshal, Phys. Rev. 80, 939 (1950).

47. J. DeJuren and B. J. Moyer, Phys. Rev. 81, 919 (1951).

48. J. A. Hofmann and K. Strauch, Phys. Rev. 90, 449 (1953).

49. F. A. Jenkins and H. E. White, Fundamentals of Physical Optics, (McGraw-Hill Book Co.), 123.

50. A. Bratenahl, S. Fernbach, R. H. Hildebrand, C. E. Leith and B. J. Moyer, Phys. Rev. 77, 597 (1950).

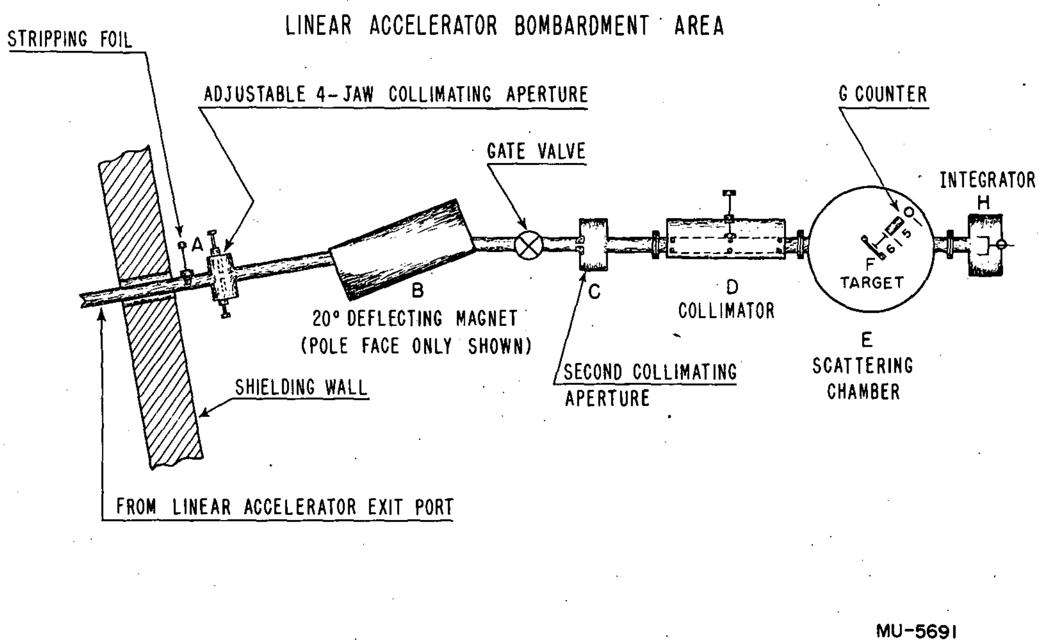

Fig. 1. Schematic of the bombardment area

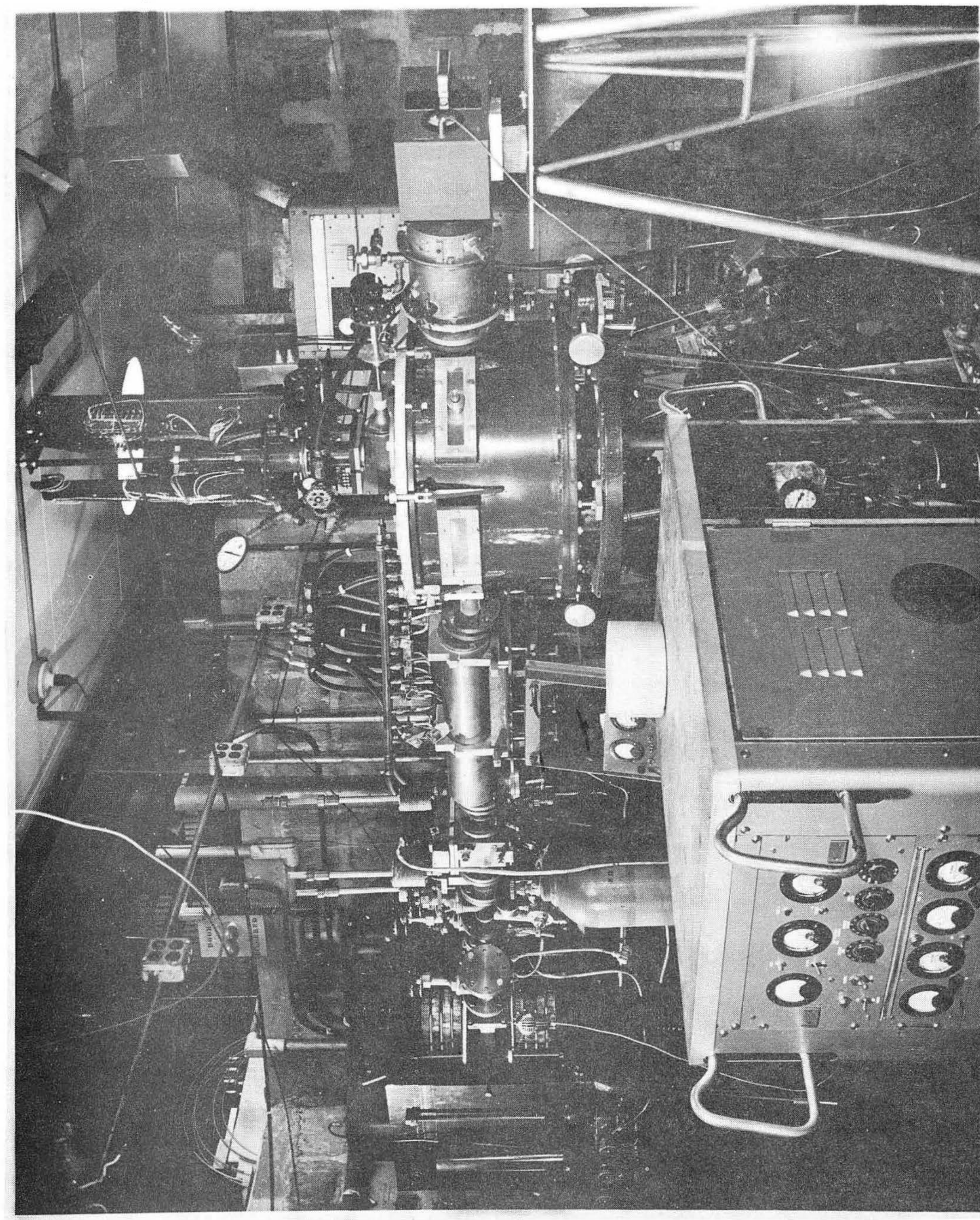

Fig. 2a. The bombardment area

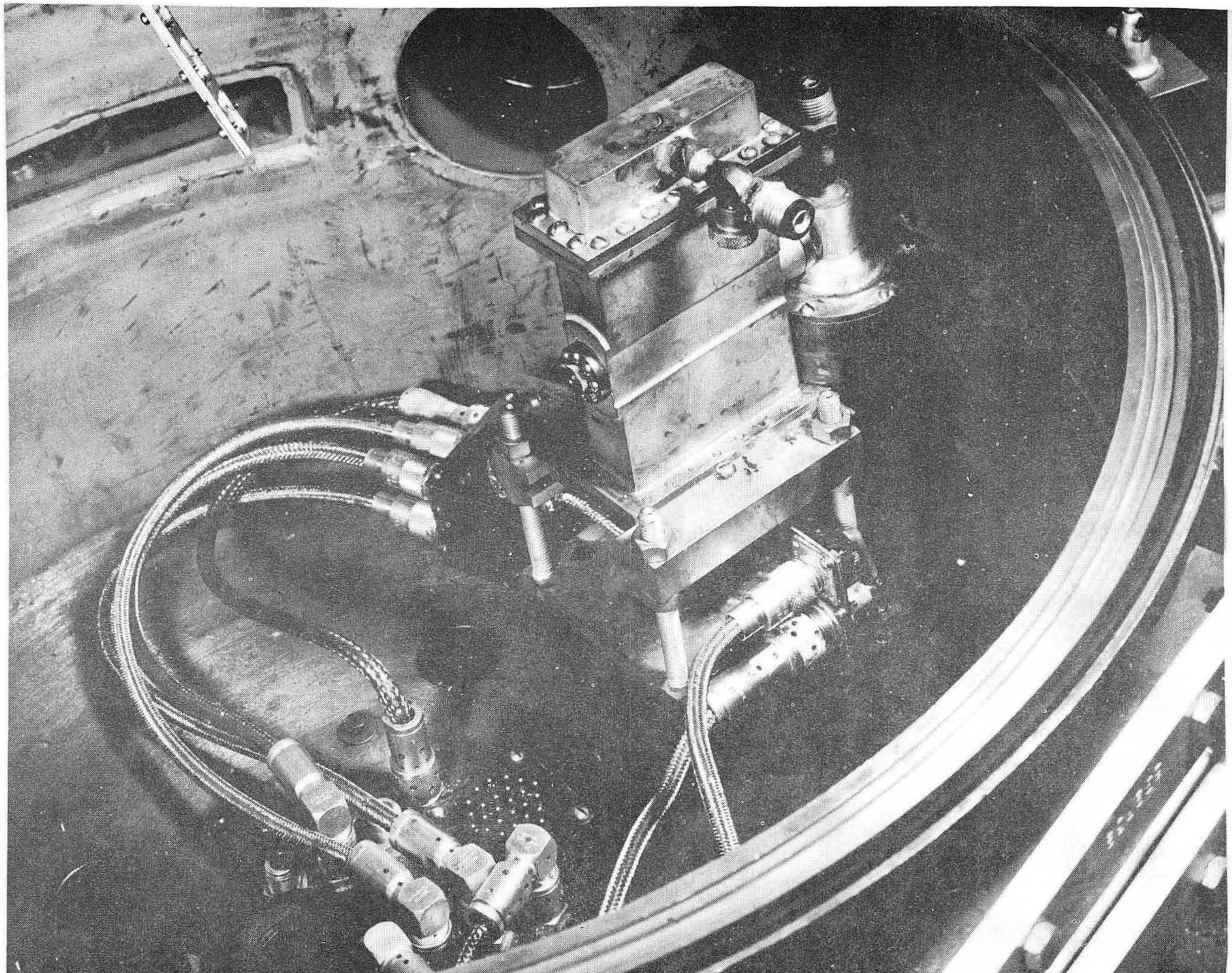

ZN-638

Fig. 2b. The counter telescope mounted on the scattering chamber table

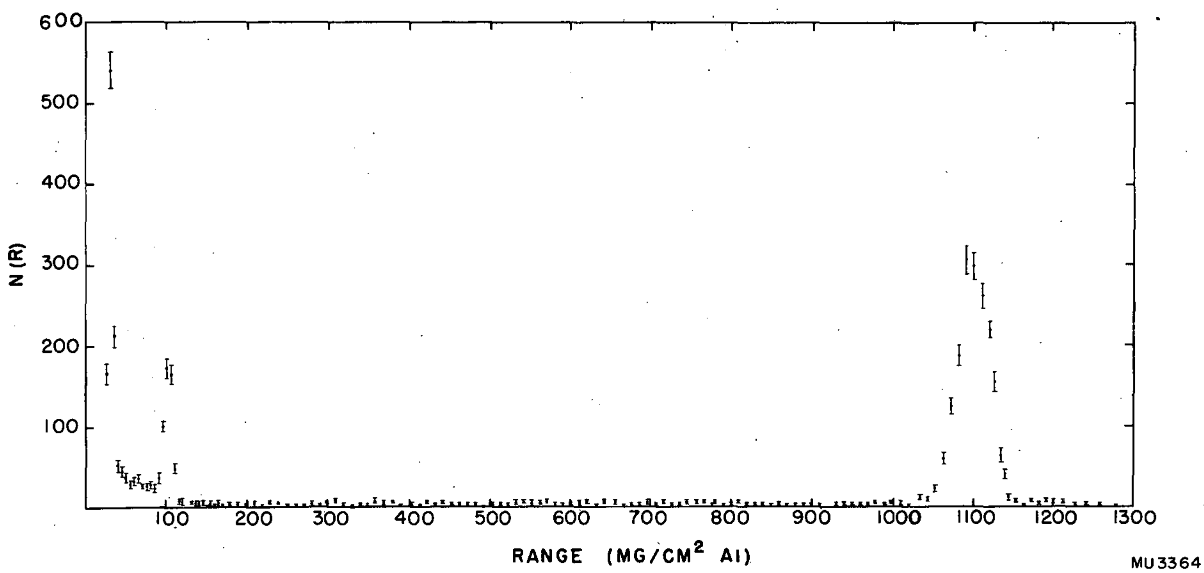

Fig. 3 Range spectrum of charged particles observed from a He target

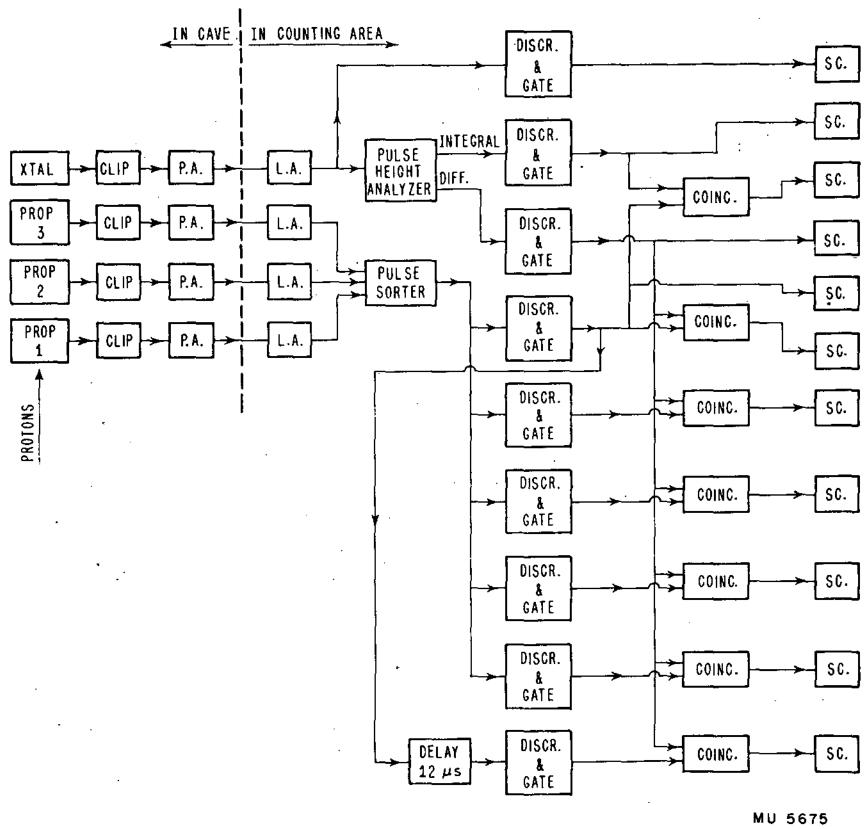

Fig. 4. Schematic of first electronic arrangement

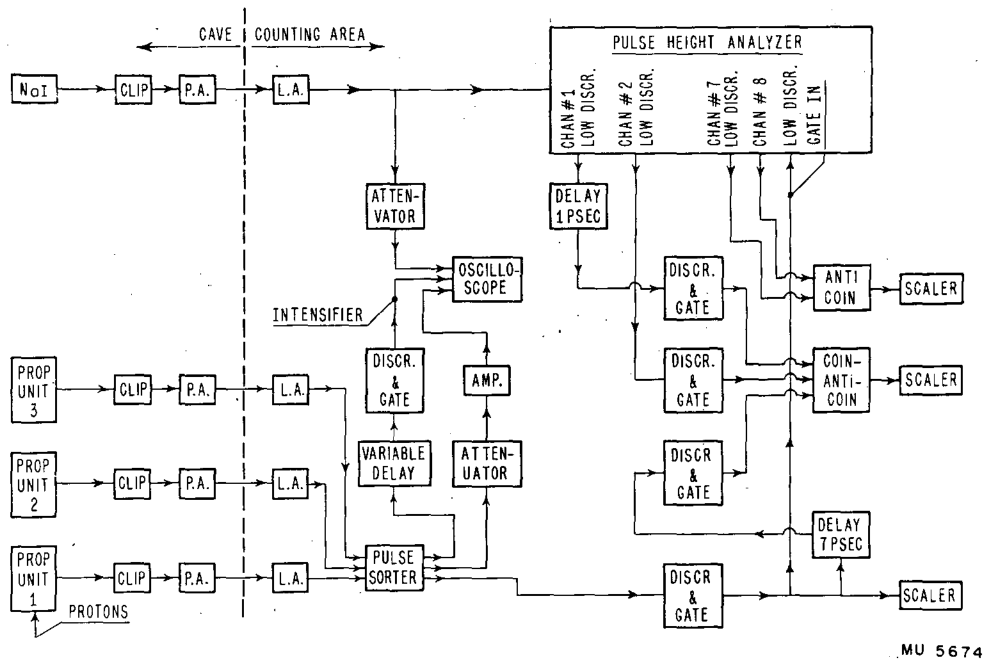

Fig. 5. Schematic of second electronic arrangement

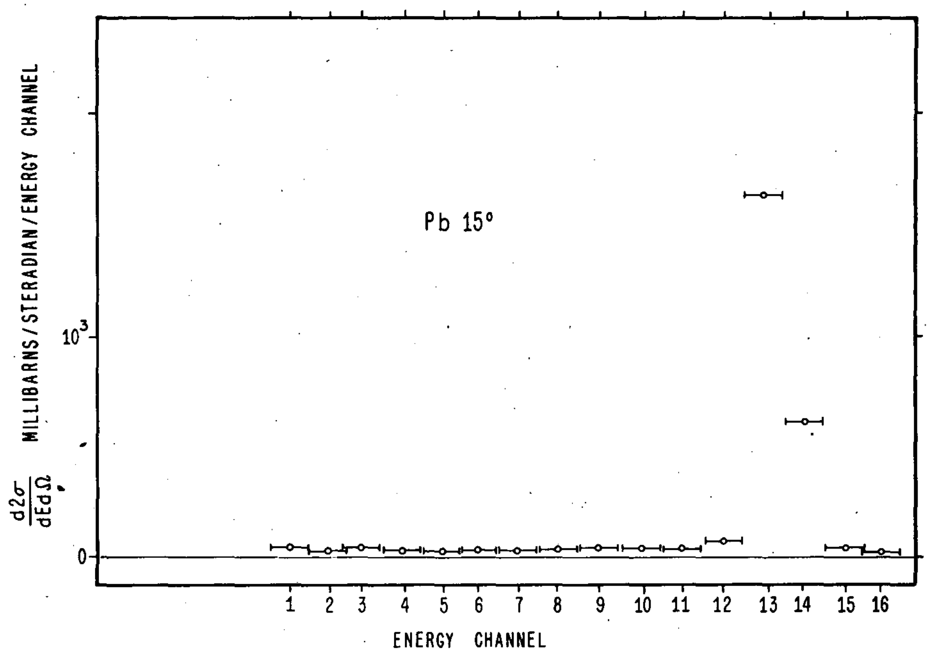

MU-5684

Fig. 6. Spectrum of particles emitted by a thin Pb target observed at a scattering angle of 15°

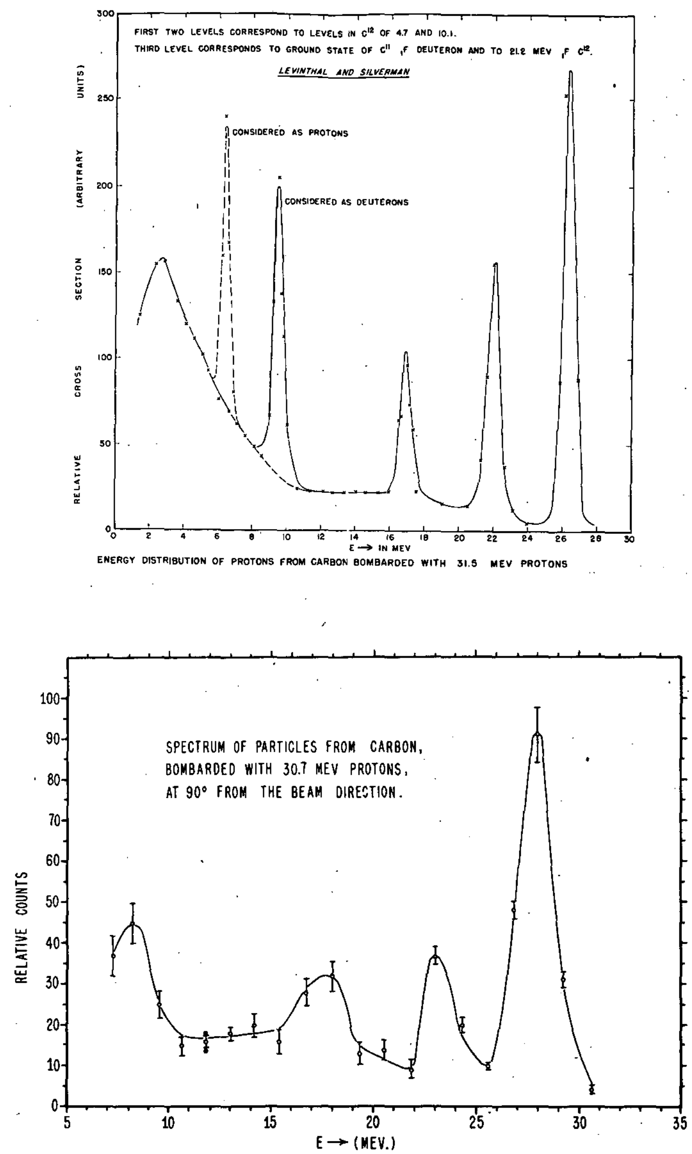

MU-5692

Fig. 7. Spectrum of particles scattered from aluminum at 90°.

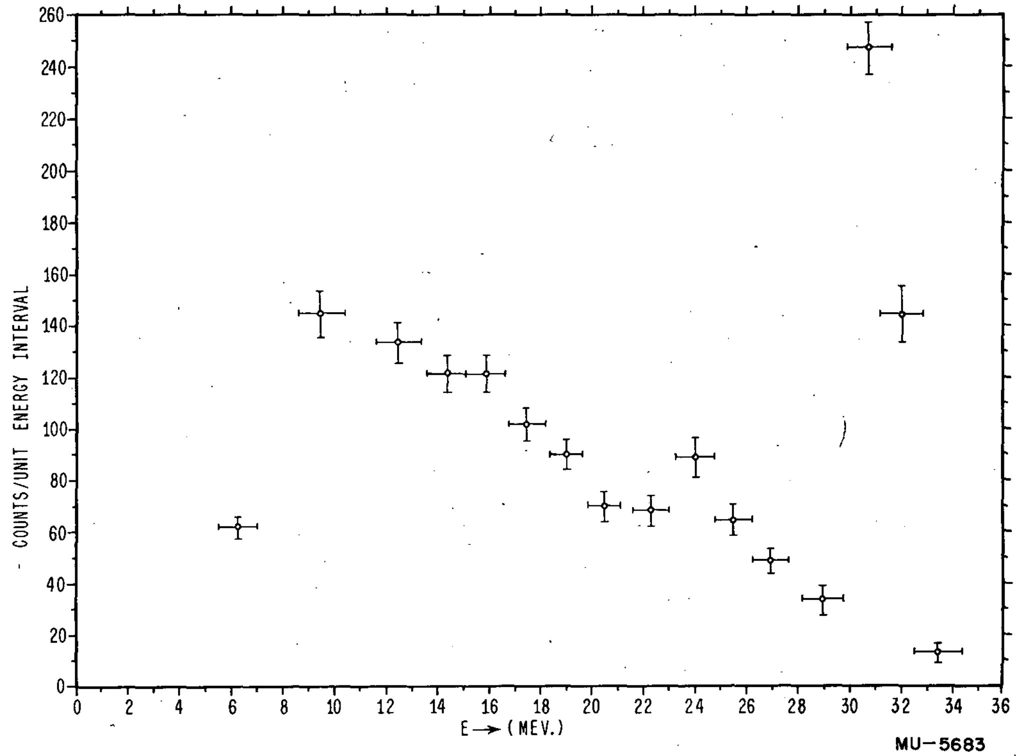

Fig. 8 Energy spectrum of heavy, charged particles emitted at 90 degrees from Pb. Data taken Oct., 1952

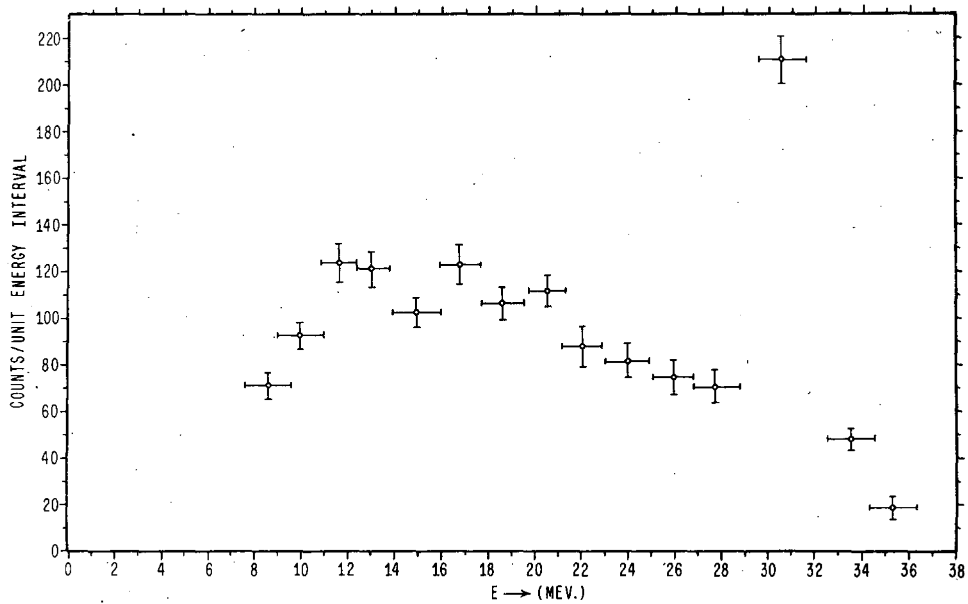

MU 5678

Fig. 9. Energy spectrum of heavy, charged particles emitted at 90 degrees from a Pb target. Data taken May, 1953

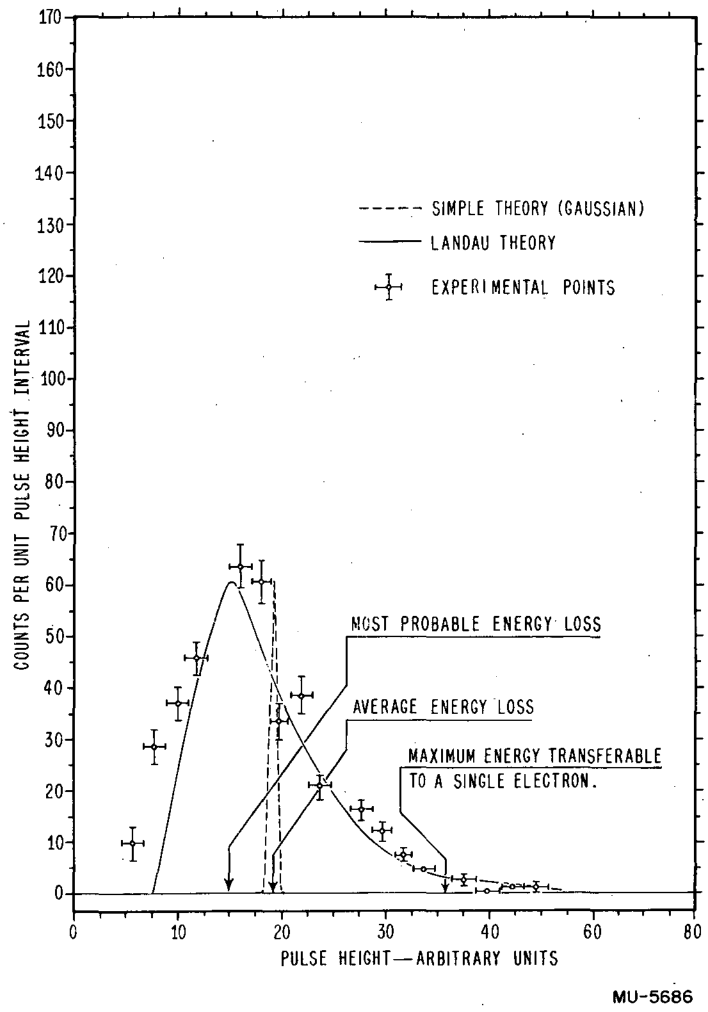

Fig. 10. Frequency distribution of energy losses of 30.5 Mev protons traversing the first unit of the triproportional counter. Histogram of experimental points show standard deviations and channel widths. The theoretical Landau distribution is computed from Symon (reference 45 The dashed curve is a Gaussian distribution based on ion pair statistics.

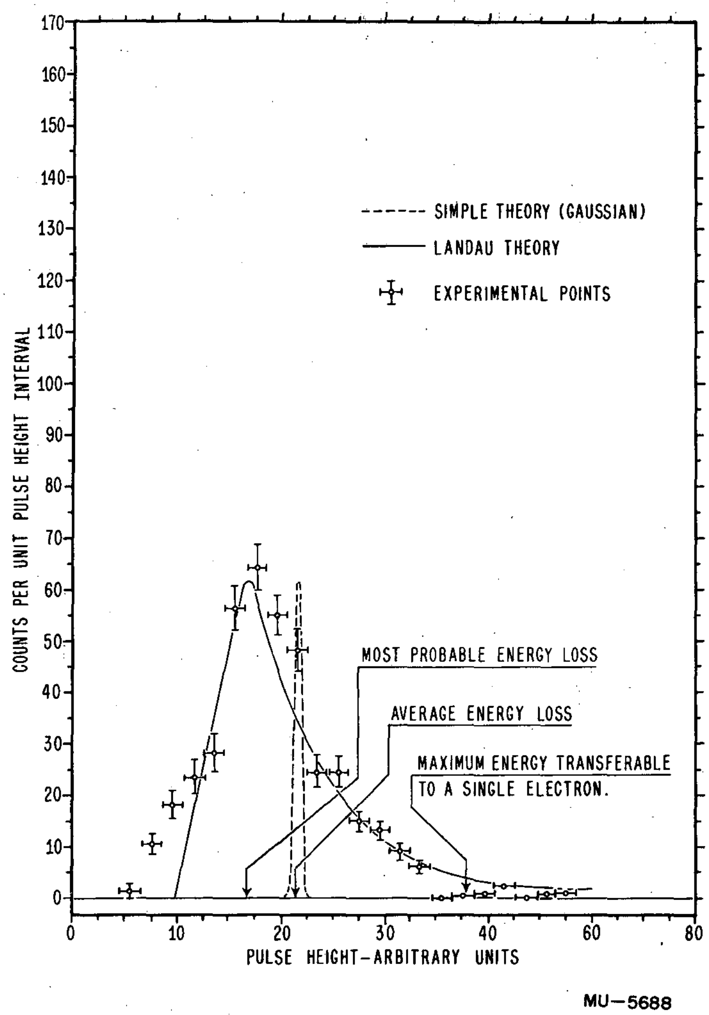

Fig. 11. Frequency distribution of energy losses of 30.5 Mev protons traversing the second unit of the triproportional counter.

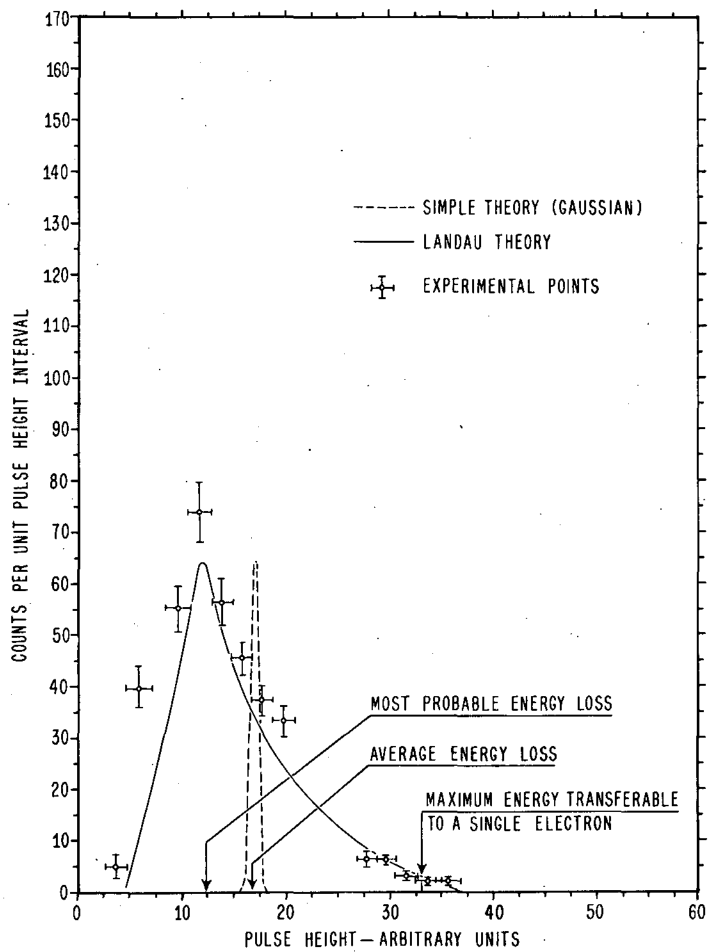

MU-5689

Fig. 12. Frequency distribution of energy losses of 30.6 Mev protons traversing the third unit of the triproportional counter

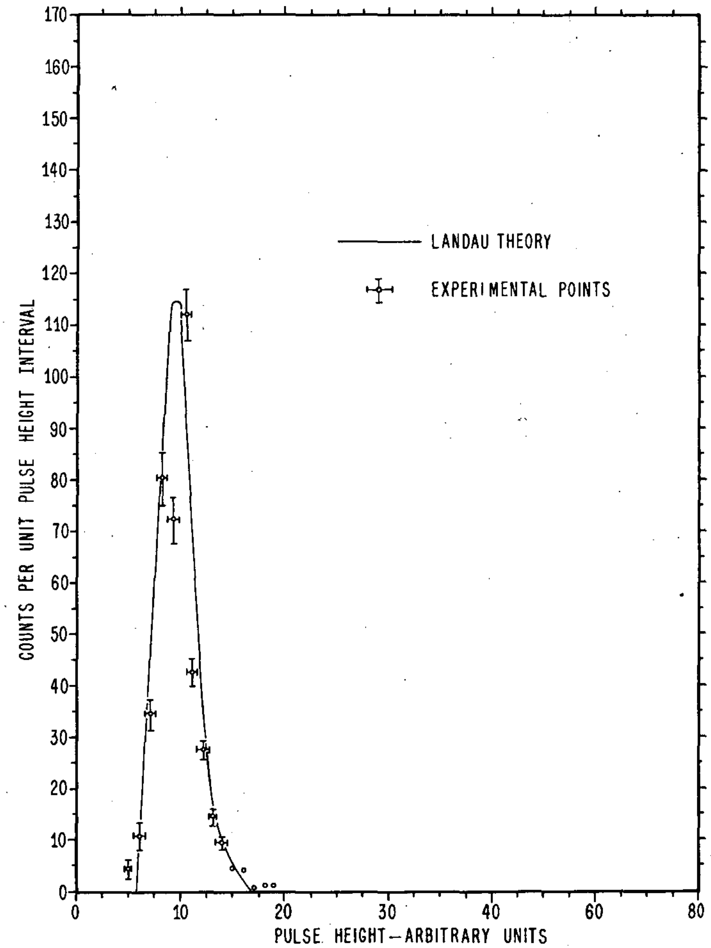

MU-5687

Fig. 13. Frequency distribution of the smallest of the three energy losses of a 30.5 Mev proton traversing the triproportional counter.

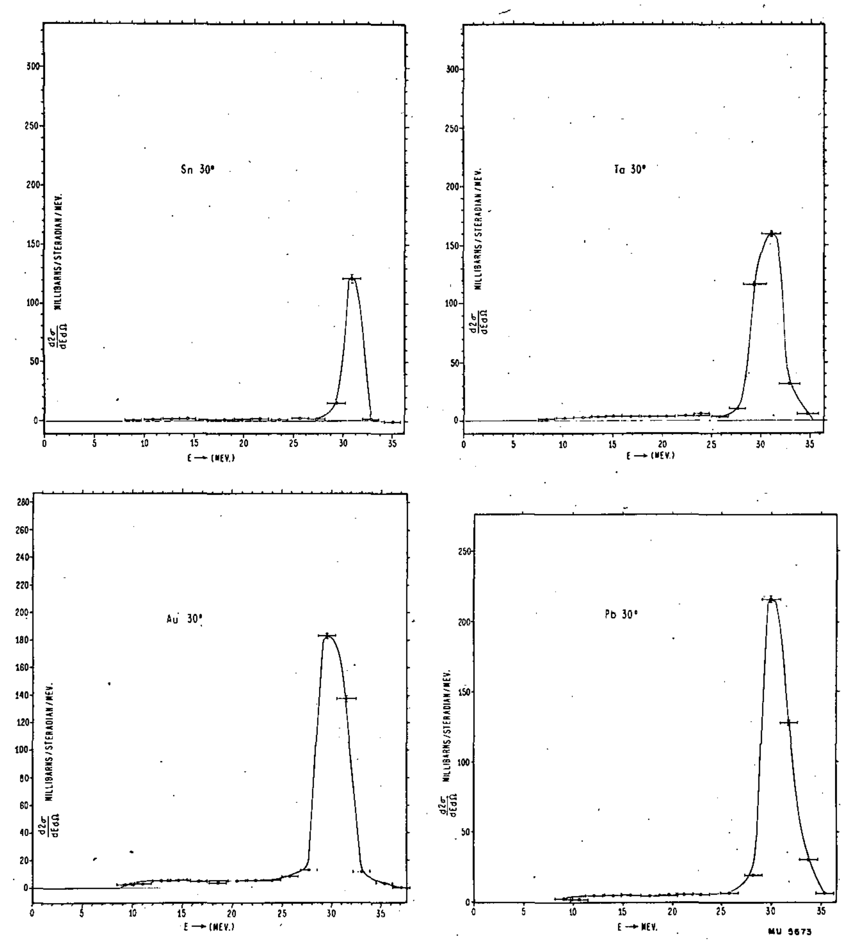

Fig. 14. Energy spectra of particles emitted by four heavy elements bombarded by 31 Mev protons at 30 degrees.

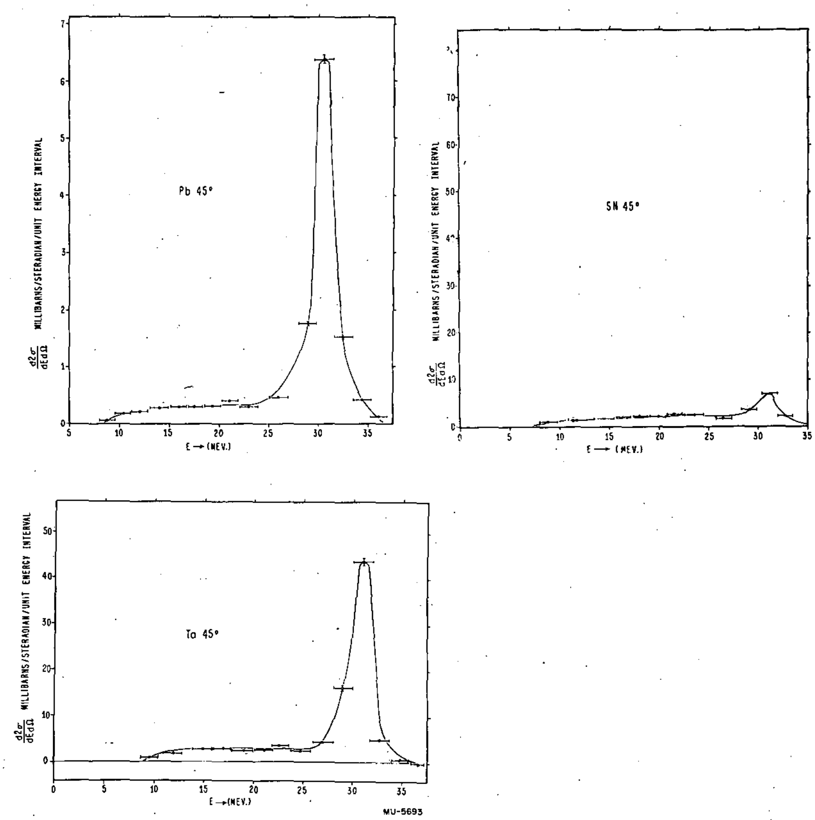

Fig. 15. Energy spectra of particles emitted by four heavy elements bombarded by 31 Mev protons at 45 degrees.

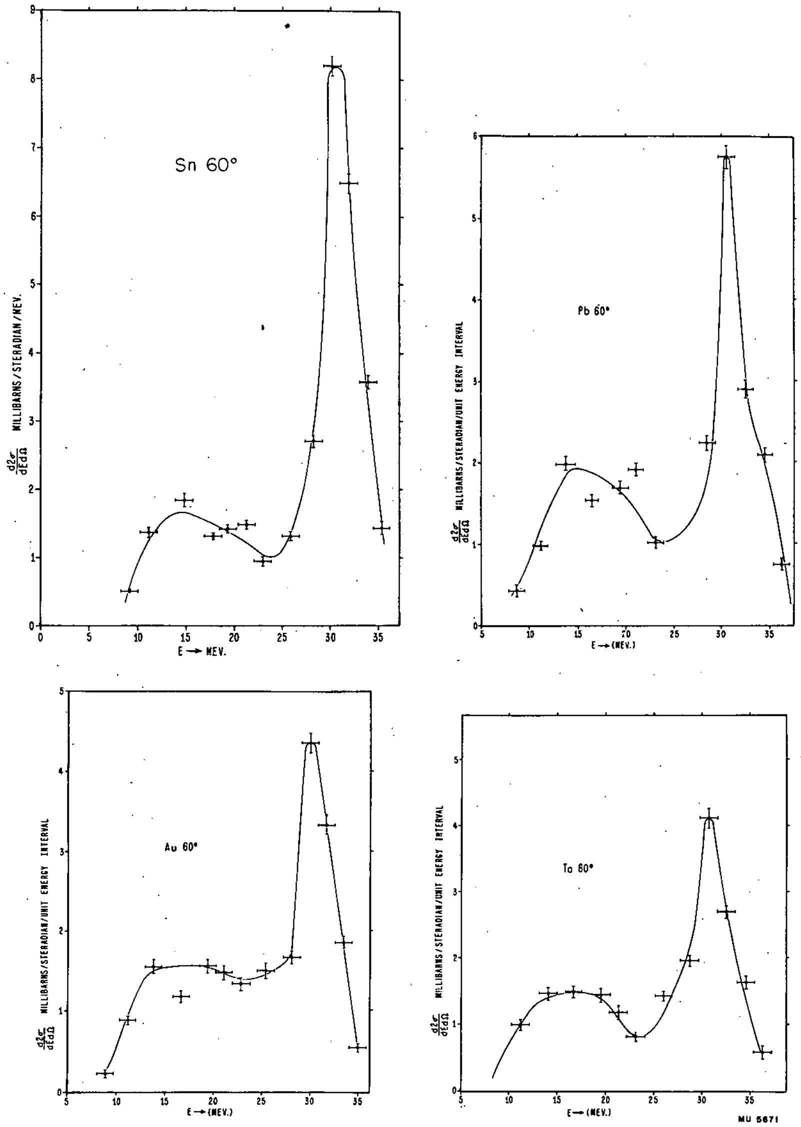

Fig. 16. Energy spectra of particles emitted by four heavy elements bombarded by 31 Mev protons at 60 degrees.

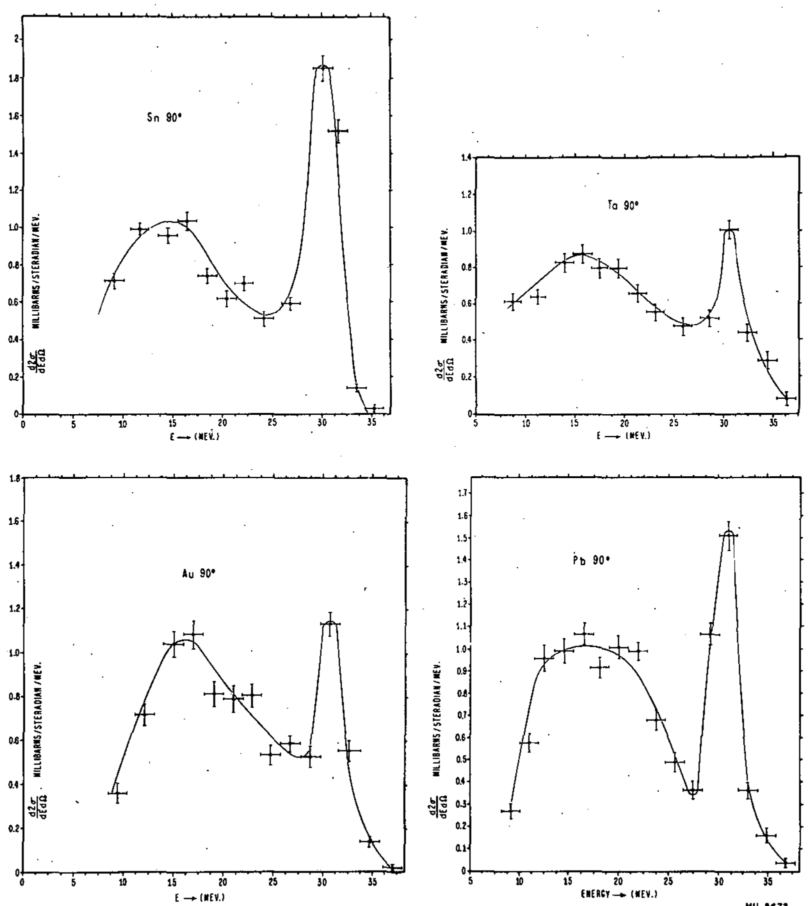

Fig. 17. Energy spectra of particles emitted by four heavy elements bombarded by 31 Mev protons at 90 degrees.

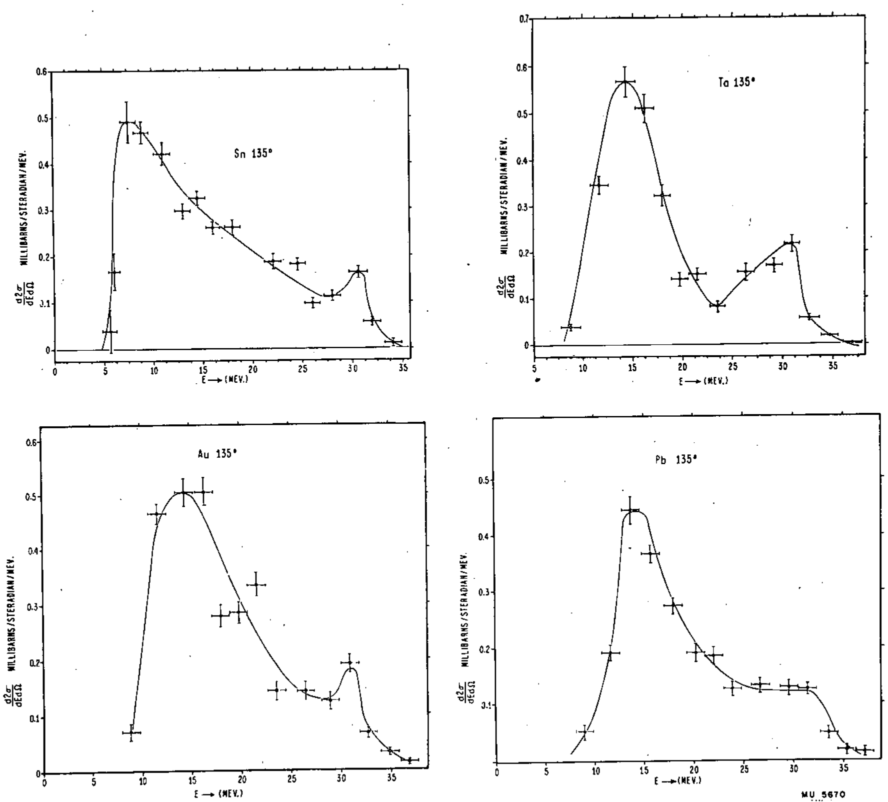

Fig. 18. Energy spectra of particles emitted by four heavy elements bombarded by 31 Mev protons at 135 degrees.

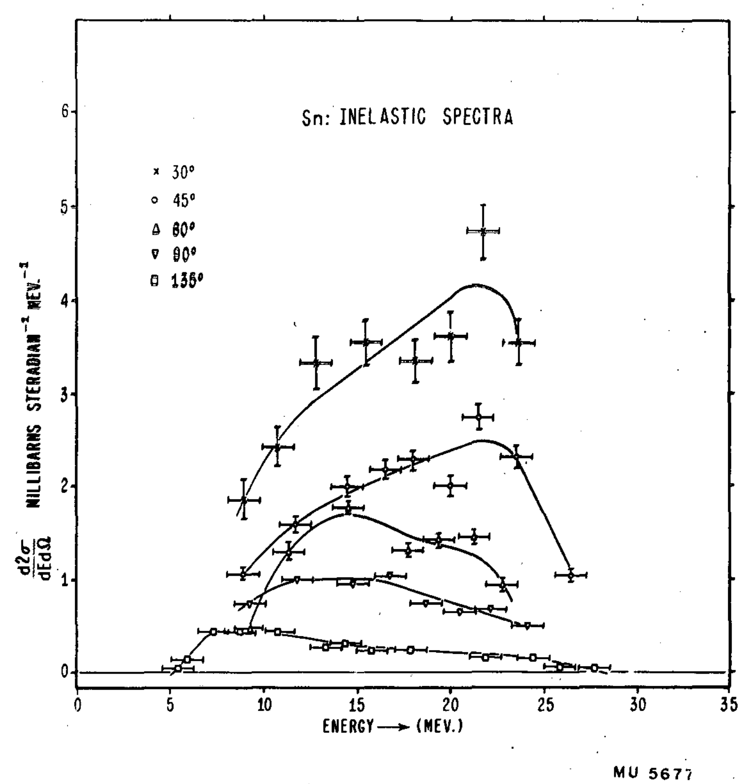

Fig. 19. Spectra of inelastically scattered particles emitted from Sn The spectra shown were taken at five scattering angles.

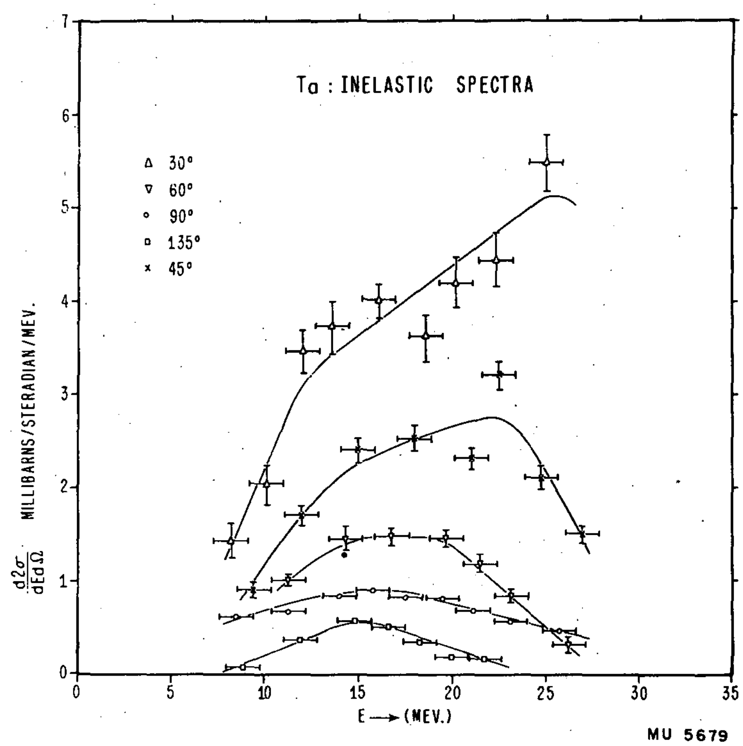

Fig. 20. Spectra of inelastically scattered particles emitted from Ta. The spectra shown were taken at five scattering angles.

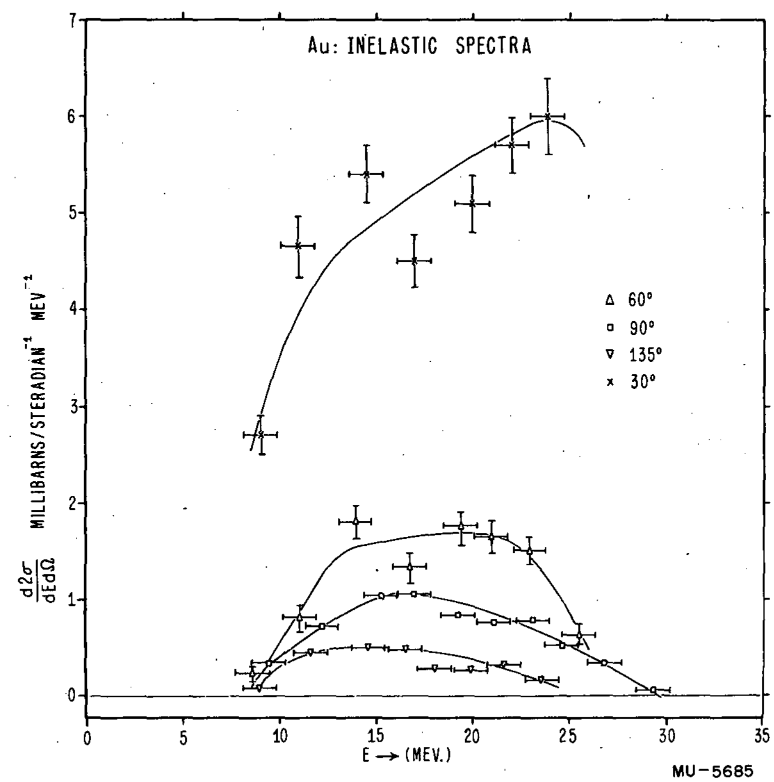

Fig. 21. Spectra of inelastically scattered particles emitted from Au. The spectra shown were taken at five scattering angles.

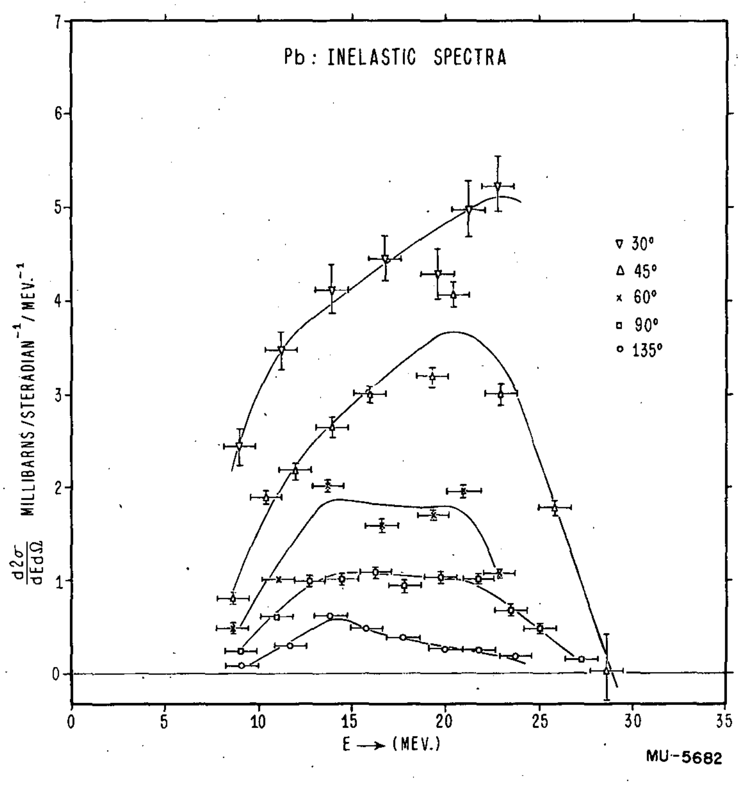

Fig. 22. Spectra of inelastically scattered particles emitted from Pb. The spectra shown were taken at five scattering angles.

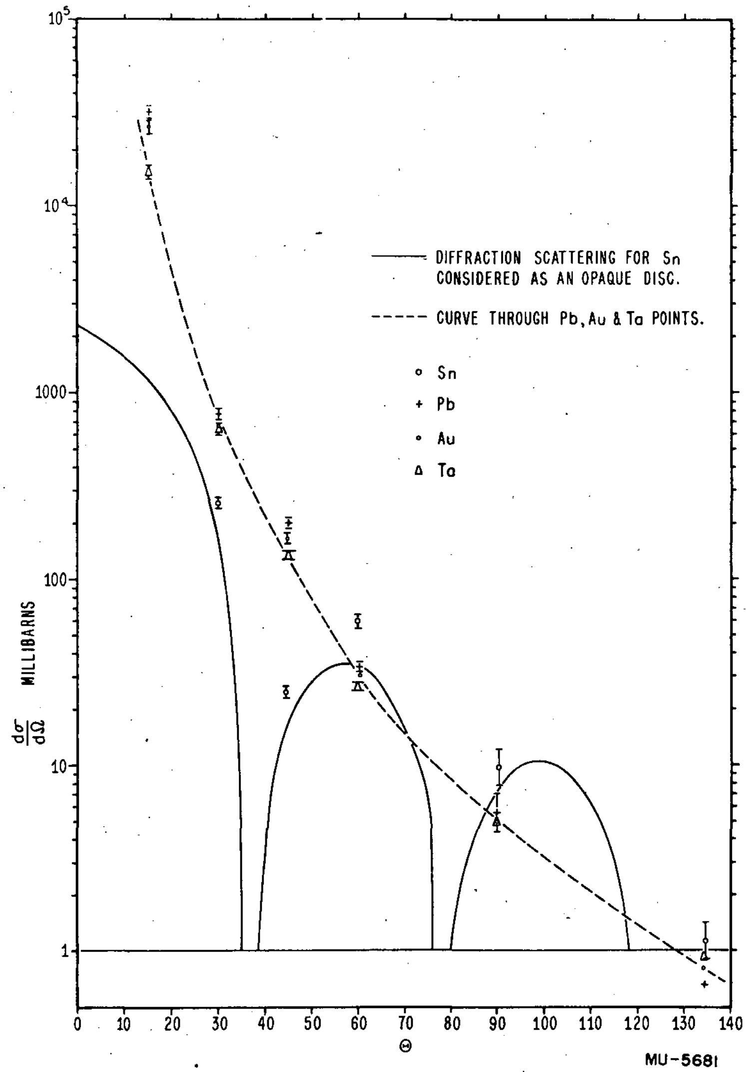

Fig. 23. The differential cross section for elastic scattering of 31 Mev protons from Sn, Pb, Au, and Ta.

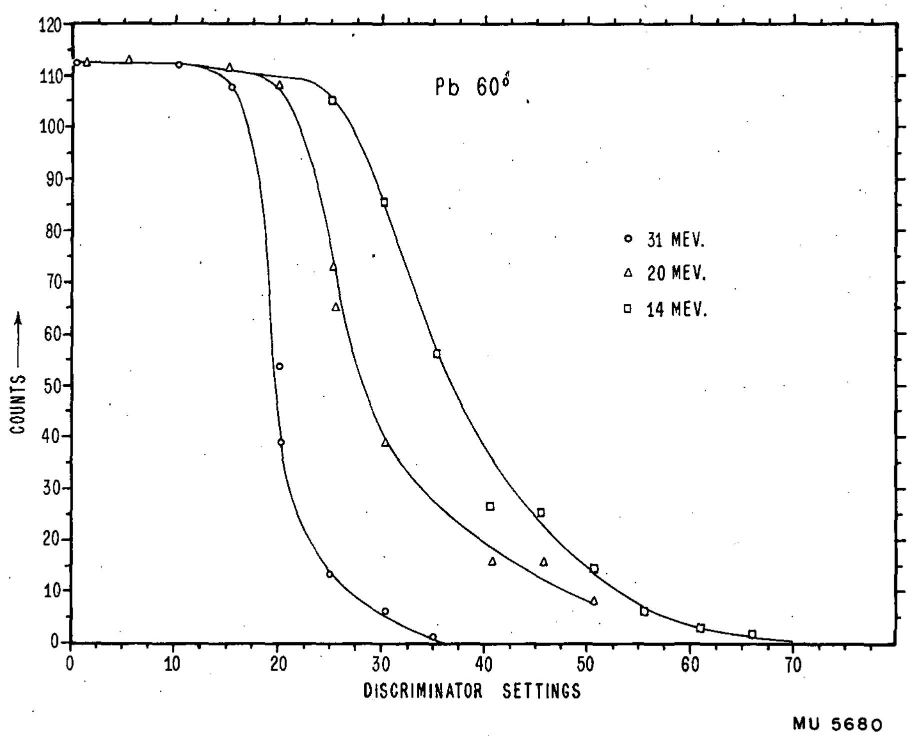

Fig. 24. Voltage discriminator plateaus on the smallest energy loss of three energy losses suffered by an energetic particle passing through the triproportional counter.

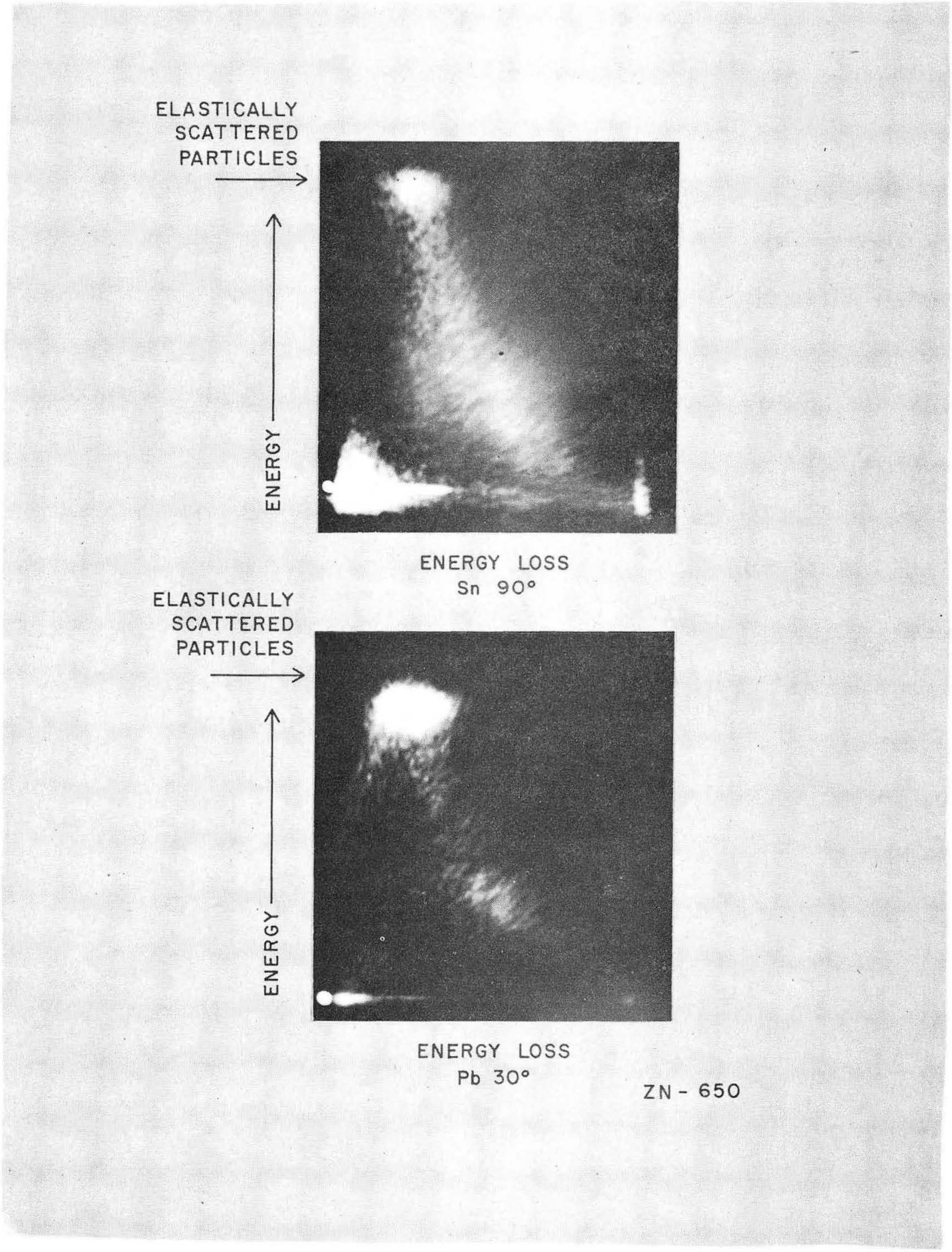

Fig. 25 Photograph of oscilloscope traces when scintillation counter pulses are put on the vertical plates and triproportional counter pulses are put on the horizontal plates.

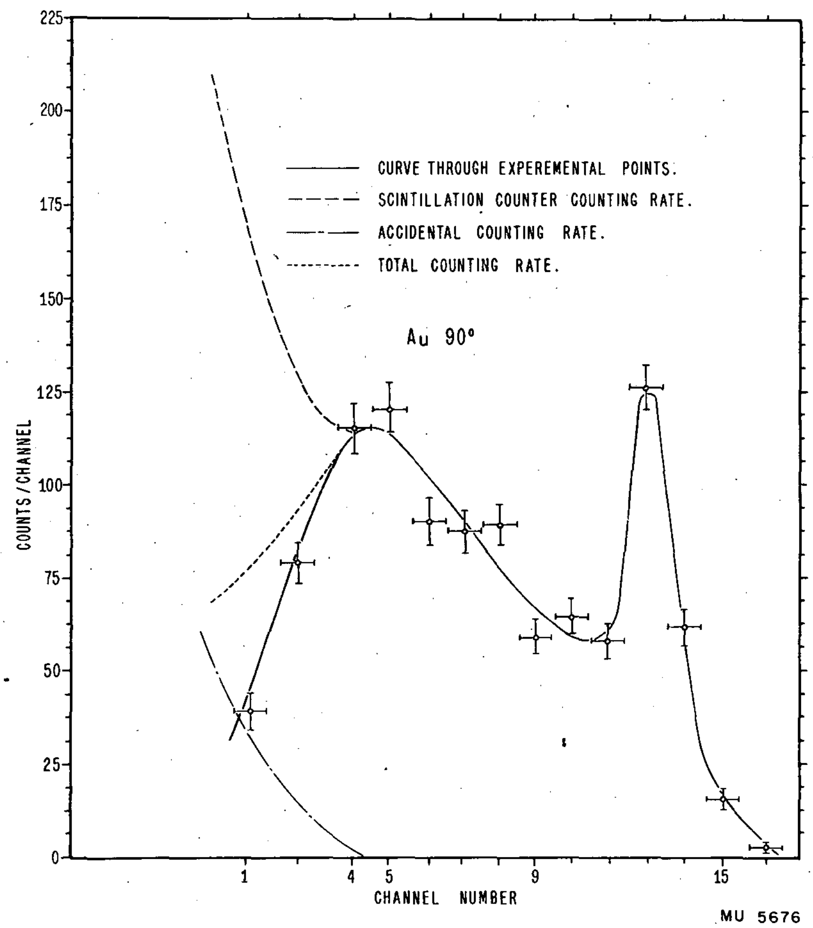

Fig. 26. Total counting rate in coincidence, scintillation counter counting rate and accidental counting rate are shown. The first two are equal in channels 5 to 16.